II. APPENDIX

Chapter 3

Table II.1: Slip rates based on geological and geodetic data for the normal faults on Crete.

Fault	**Geological data**[a]		**Geodetic data**[b]	
	Slip rate [m/ka]	**Slip rate * 13 kyr**	**Slip rate [mm/yr]**	**Slip rate * 8 kyr**
Sfakia (SfF)	1.0	13	0.97 ± 1.07	7.76 ± 8.56
Asomatos (AF)	0.6	7.8	1.01 ± 0.98	8.08 ± 7.84
Spili (SpF)	0.8	10.4	0.60 ± 1.46	4.8 ± 11.68
Gramvousa (GrF)	0.7	9.1	0.68 ± 1.13	5.44 ± 9.04
Gionas (GF)	0.3	3.9	0.40 ± 0.99	3.2 ± 7.92
Rodopos (RF)	0.3	3.9	0 05 ± 1.01	0 4 ± 8.08
Kera (KeF)	0.4	5.2	0.21 ± 0.92	1.68 ± 7.36
Kroussonas (KrF)	1.0	13	0.91 ± 0.54	7.28 ± 4.32
Agia Varvara (AVF)	0.8	10.4	2.48 ± 0.73	19.84 ± 5.84
Kastelli (KF)	0.5	6.5	0.81 ± 0.98	6.48 ± 7.84
Ha Gorge (HGF)	0.9	11.7	1.16 ± 1.80	9.28 ± 14.4
Lastros (LF)	1.3	16.9	0.49 ± 3.08	3.92 ± 24.64
Zou (ZF)	0.7	9.1	2.34 ± 2.83	18.72 ± 22.64

[a]Geological data taken from Caputo et al. (2010).
[b]Geodetic data based on my PSI analysis

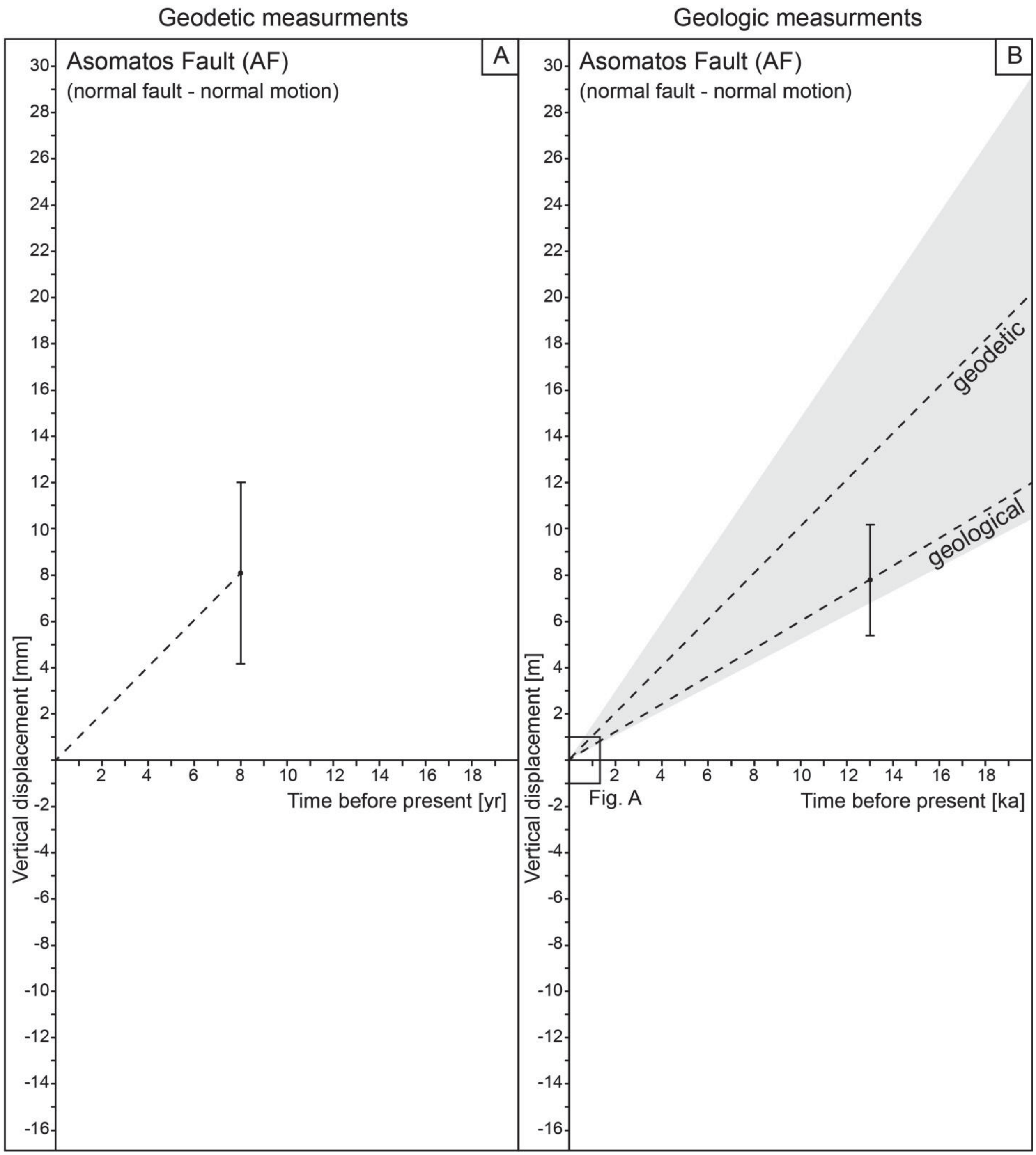

Figure II.1: A) Shows the vertical displacement in mm/yr measured by PSI along the Asomatos fault. B) Shows the geodetic measurements versus the geologic slip-rate in ka/m derived from Caputo et al. (2010). The grey shade shows the error range of PSI measurements adjusted to the geological time.

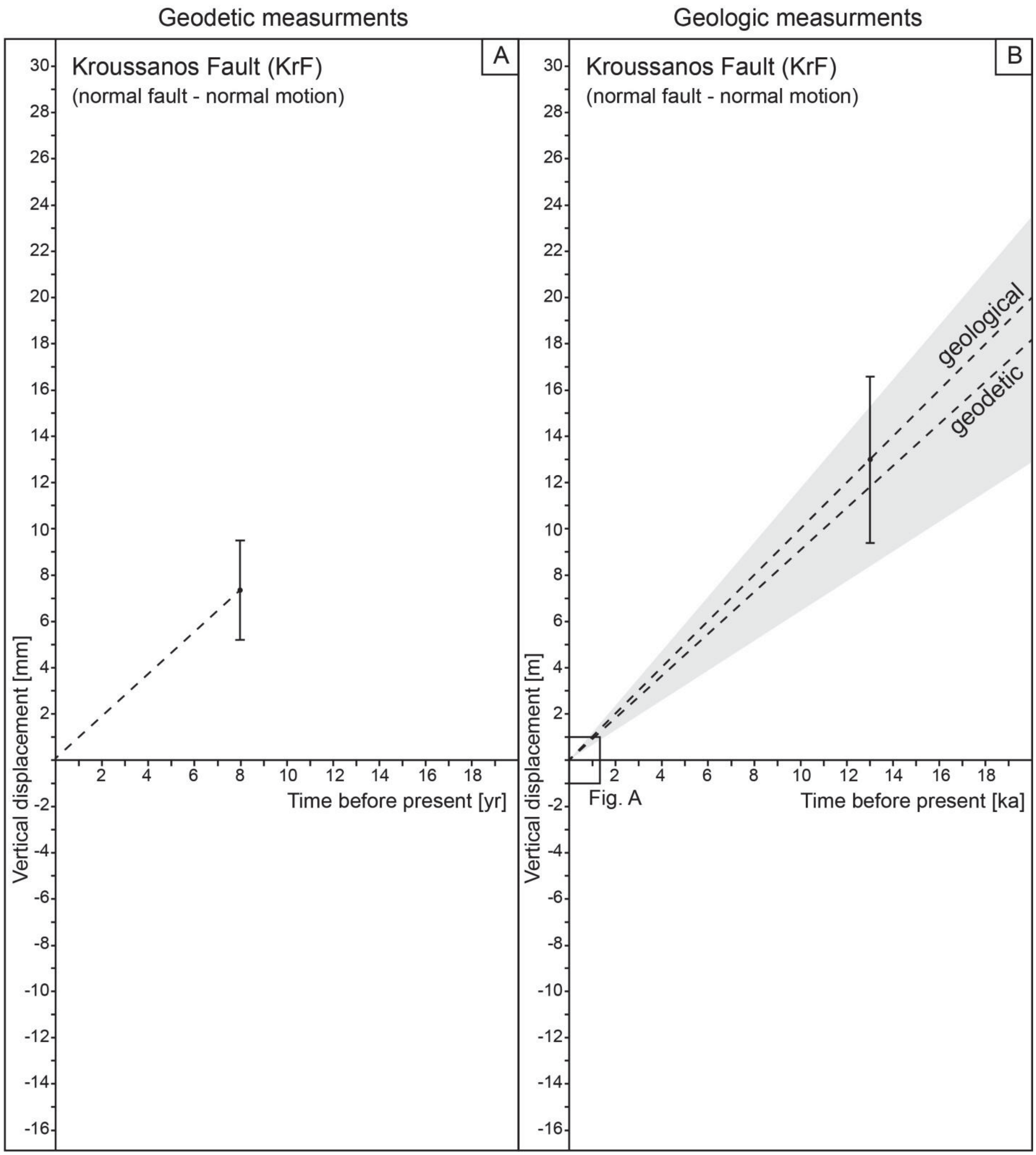

Figure II.2: A) Shows the vertical displacement in mm/yr measured by PSI along the Kroussanos fault. B) Shows the geodetic measurements versus the geologic slip-rate in ka/m derived from Caputo et al. (2010). The grey shade shows the error range of PSI measurements adjusted to the geological time.

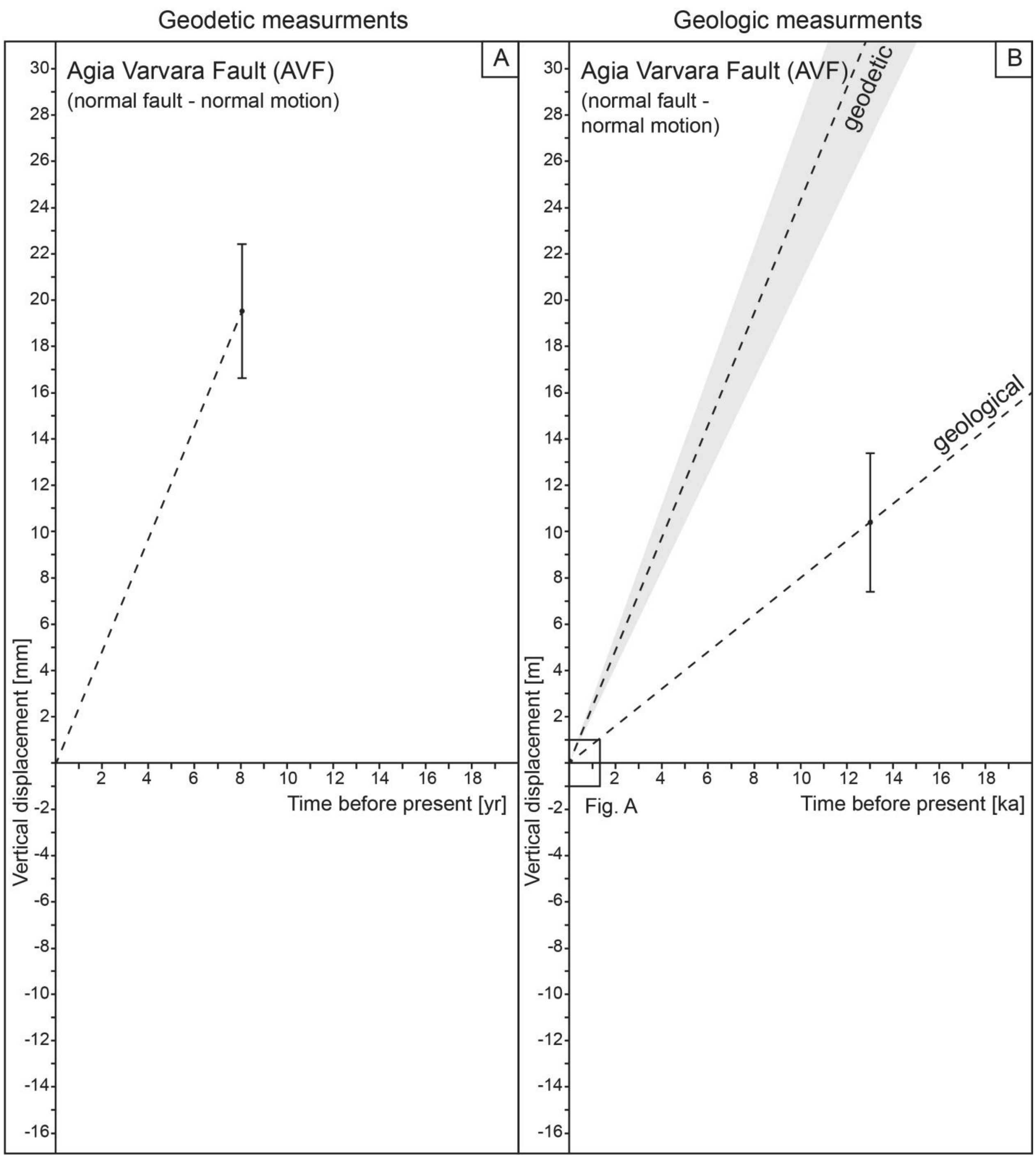

Figure II.3: a) Shows the vertical displacement in mm/yr measured by PSI along the Agia Varvara fault. B) Shows the geodetic measurements versus the geologic slip-rate in ka/m derived from Caputo et al. (2010). The grey shade shows the error range of PSI measurements adjusted to the geological time.

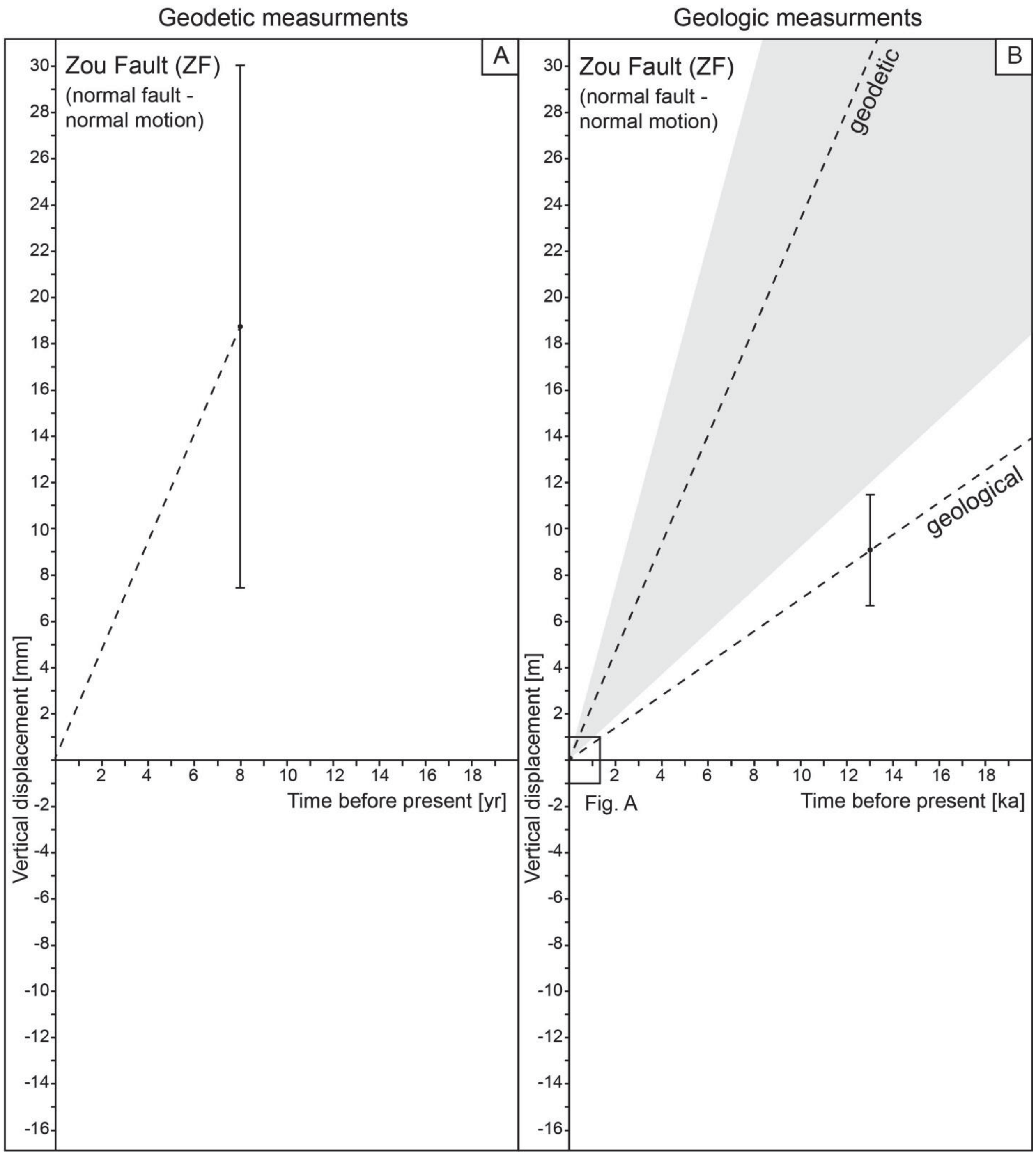

Figure II.4: A) Shows the vertical displacement in mm/yr measured by PSI along the Zou fault. B) Shows the geodetic measurements versus the geologic slip-rate in ka/m derived from Caputo et al. (2010). The grey shade shows the error range of PSI measurements adjusted to the geological time.

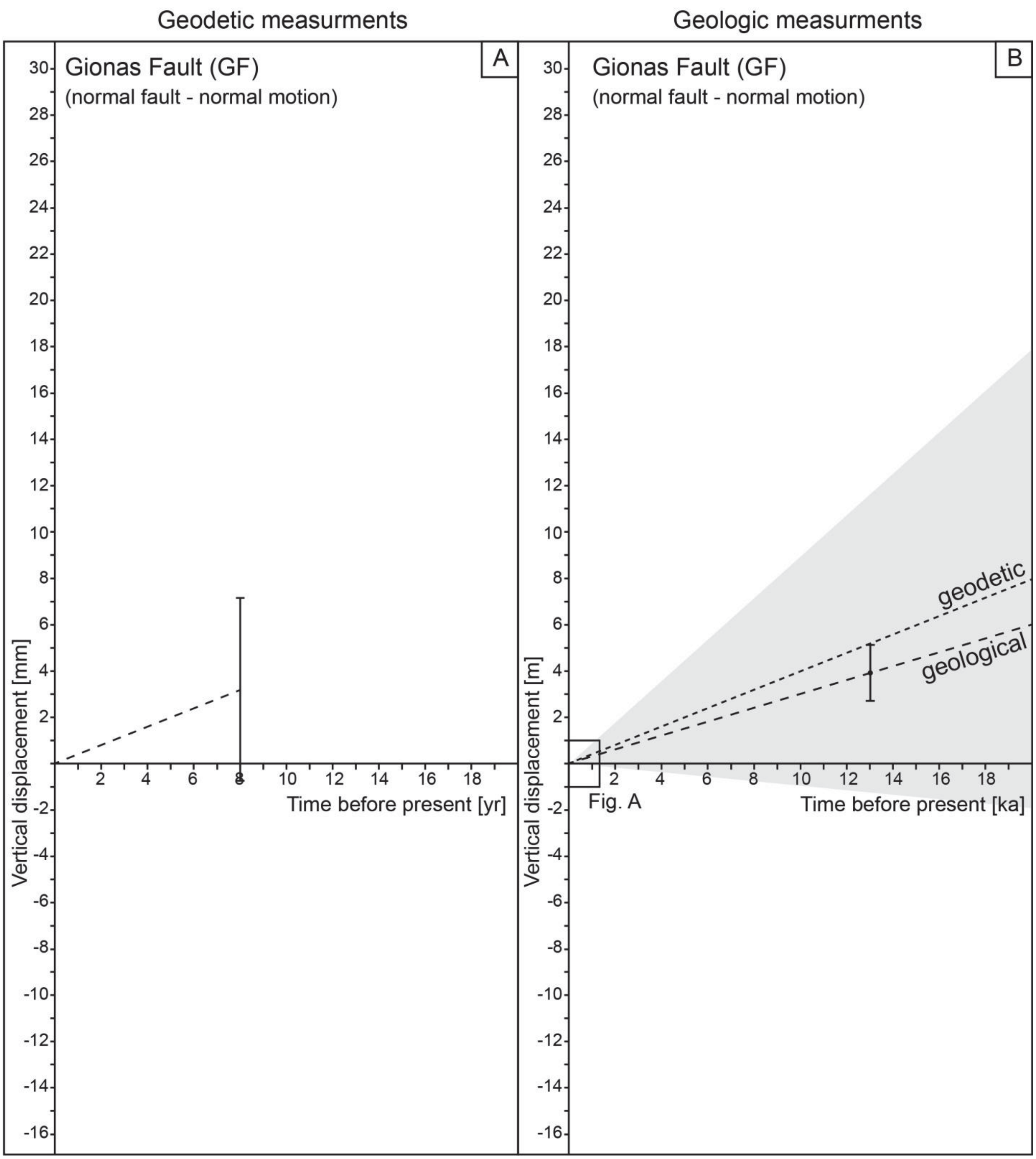

Figure II.5: A) Shows the vertical displacement in mm/yr measured by PSI along the Gionas fault. B) Shows the geodetic measurements versus the geologic slip-rate in ka/m derived from Caputo et al. (2010). The grey shade shows the error range of PSI measurements adjusted to the geological time.

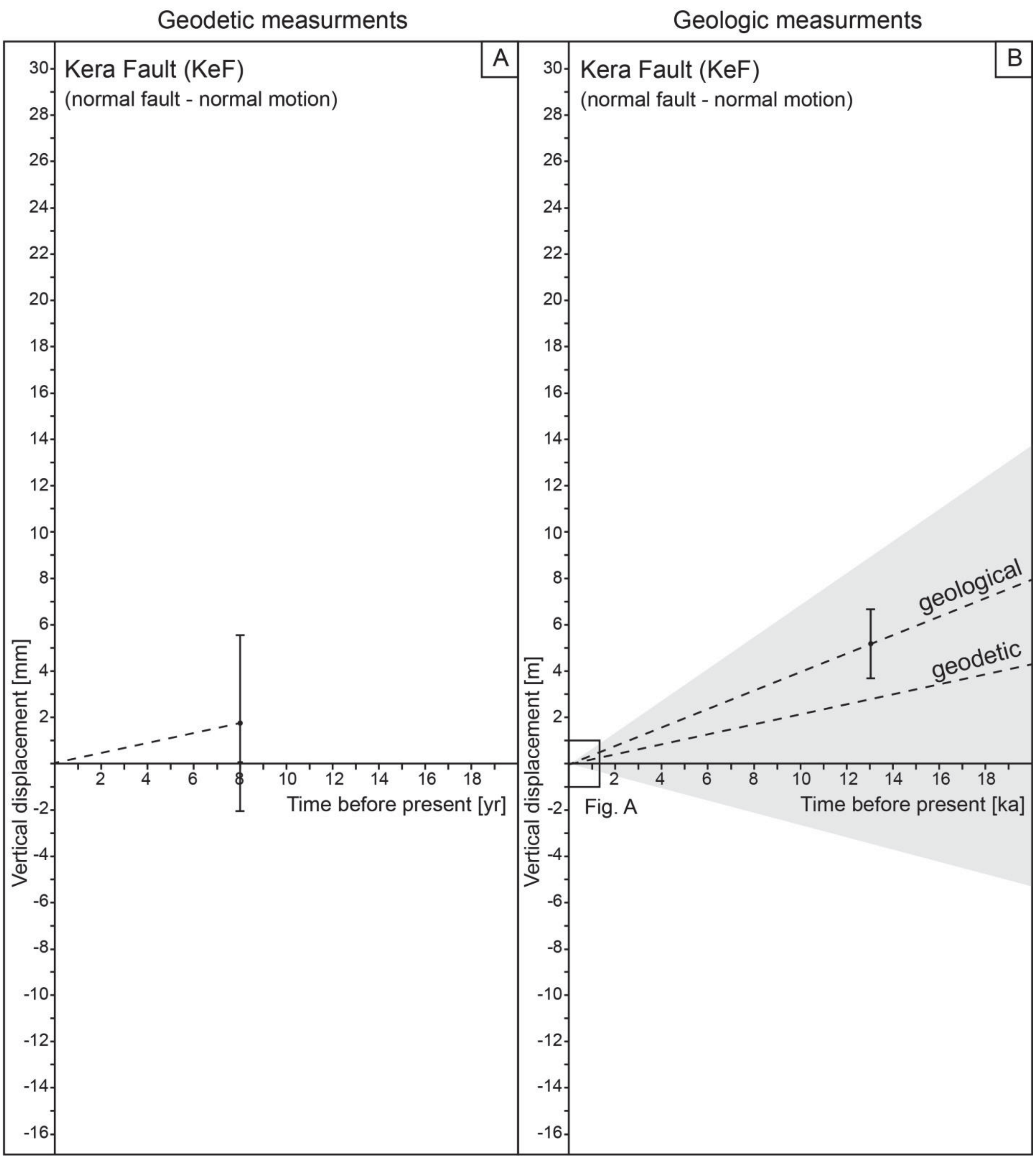

Figure II.6: A) Shows the vertical displacement in mm/yr measured by PSI along the Kera fault. B) Shows the geodetic measurements versus the geologic slip-rate in ka/m derived from Caputo et al. (2010). The grey shade shows the error range of PSI measurements adjusted to the geological time.

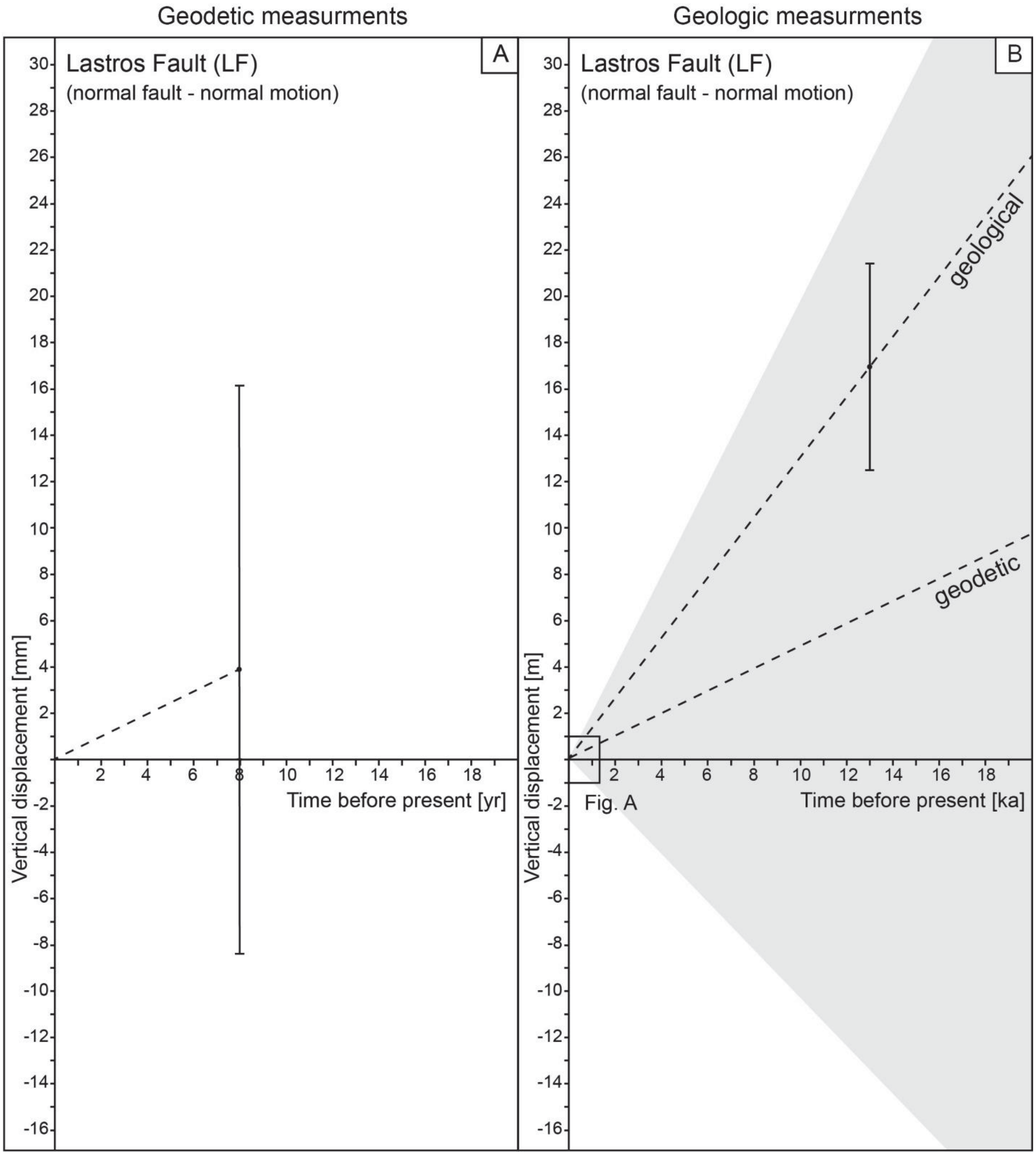

Figure II.7: A) Shows the vertical displacement in mm/yr measured by PSI along the Lastros fault. B) Shows the geodetic measurements versus the geologic slip-rate in ka/m derived from Caputo et al. (2010). The grey shade shows the error range of PSI measurements adjusted to the geological time.

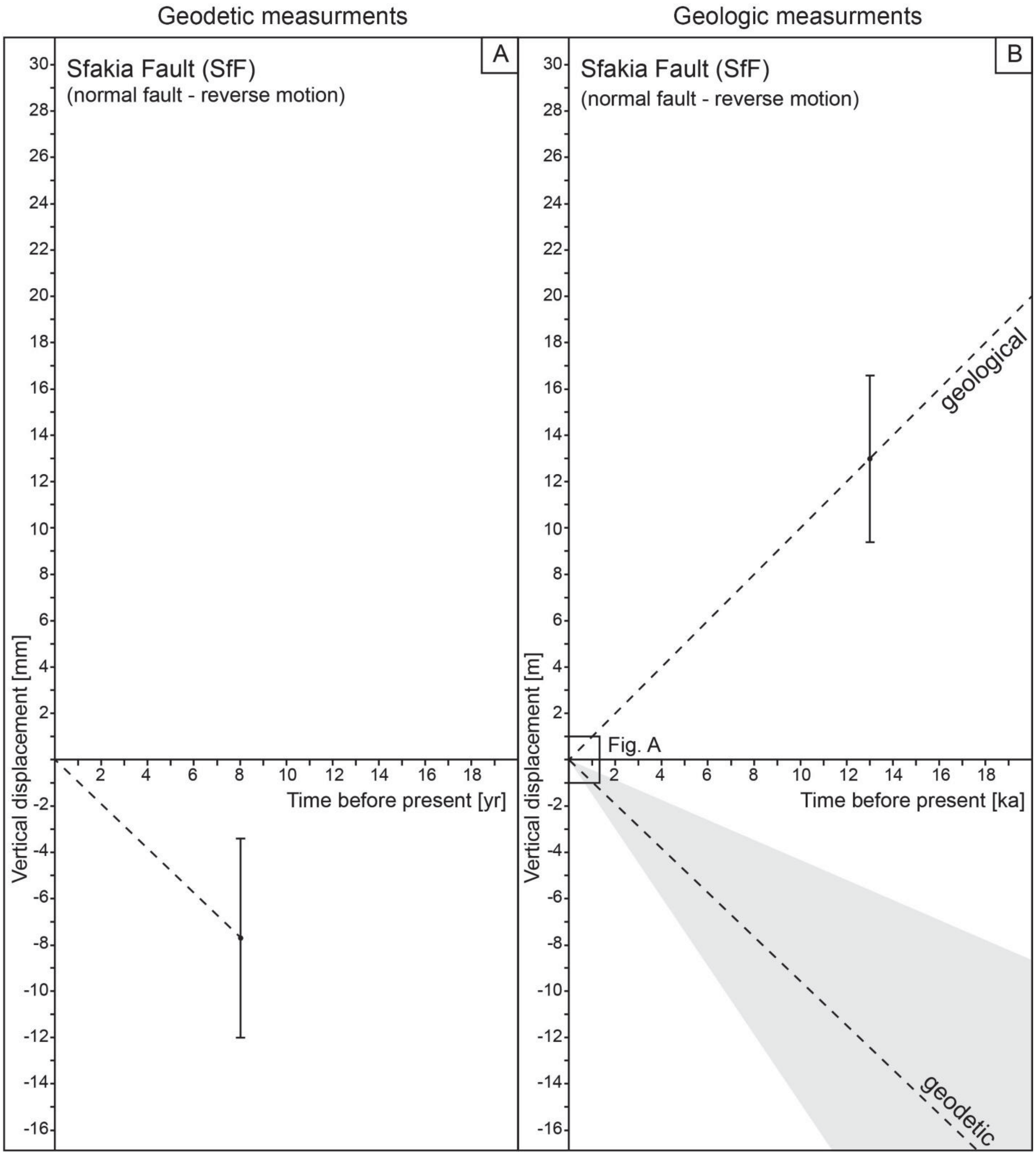

Figure II.8: A) Shows the vertical displacement in mm/yr measured by PSI along the Sfakia fault. B) Shows the geodetic measurements versus the geologic slip-rate in ka/m derived from Caputo et al. (2010). The grey shade shows the error range of PSI measurements adjusted to the geological time.

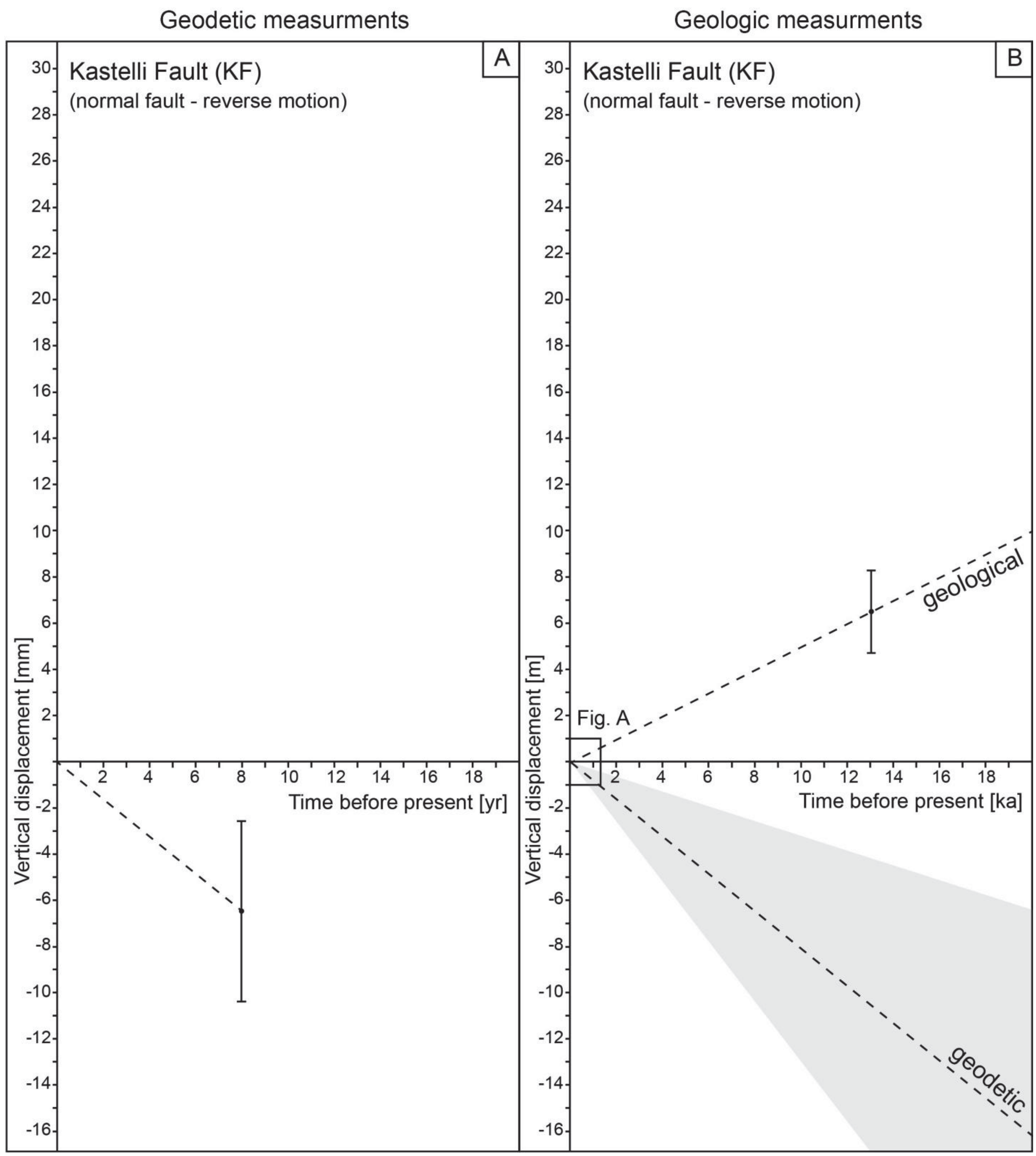

Figure II.9: A) Shows the vertical displacement in mm/yr measured by PSI along the Kastelli fault. B) Shows the geodetic measurements versus the geologic slip-rate in ka/m derived from Caputo et al. (2010). The grey shade shows the error range of PSI measurements adjusted to the geological time.

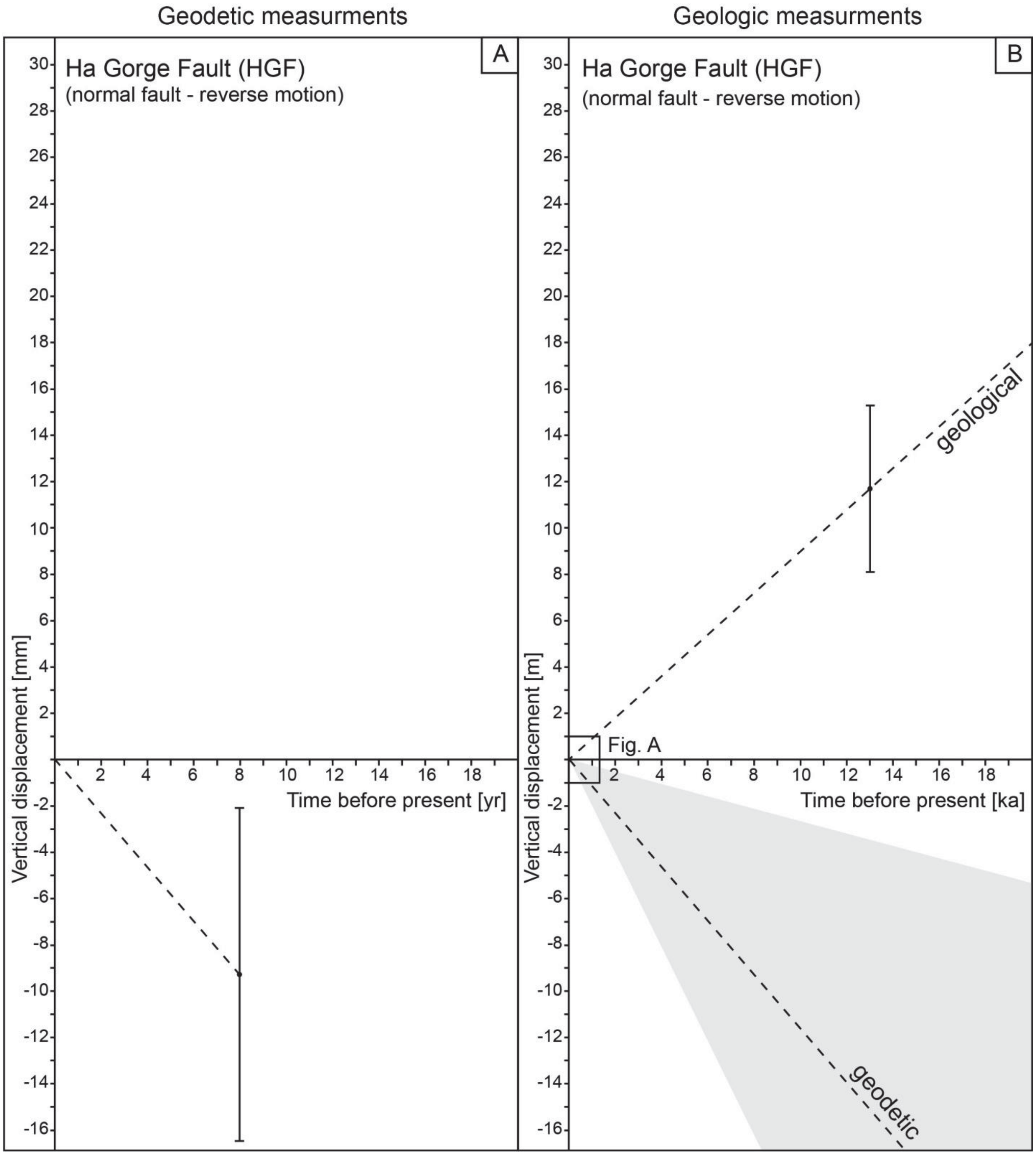

Figure II.10: A) Shows the vertical displacement in mm/yr measured by PSI along the Ha Gorge fault. B) Shows the geodetic measurements versus the geologic slip-rate in ka/m derived from Caputo et al. (2010). The grey shade shows the error range of PSI measurements adjusted to the geological time.

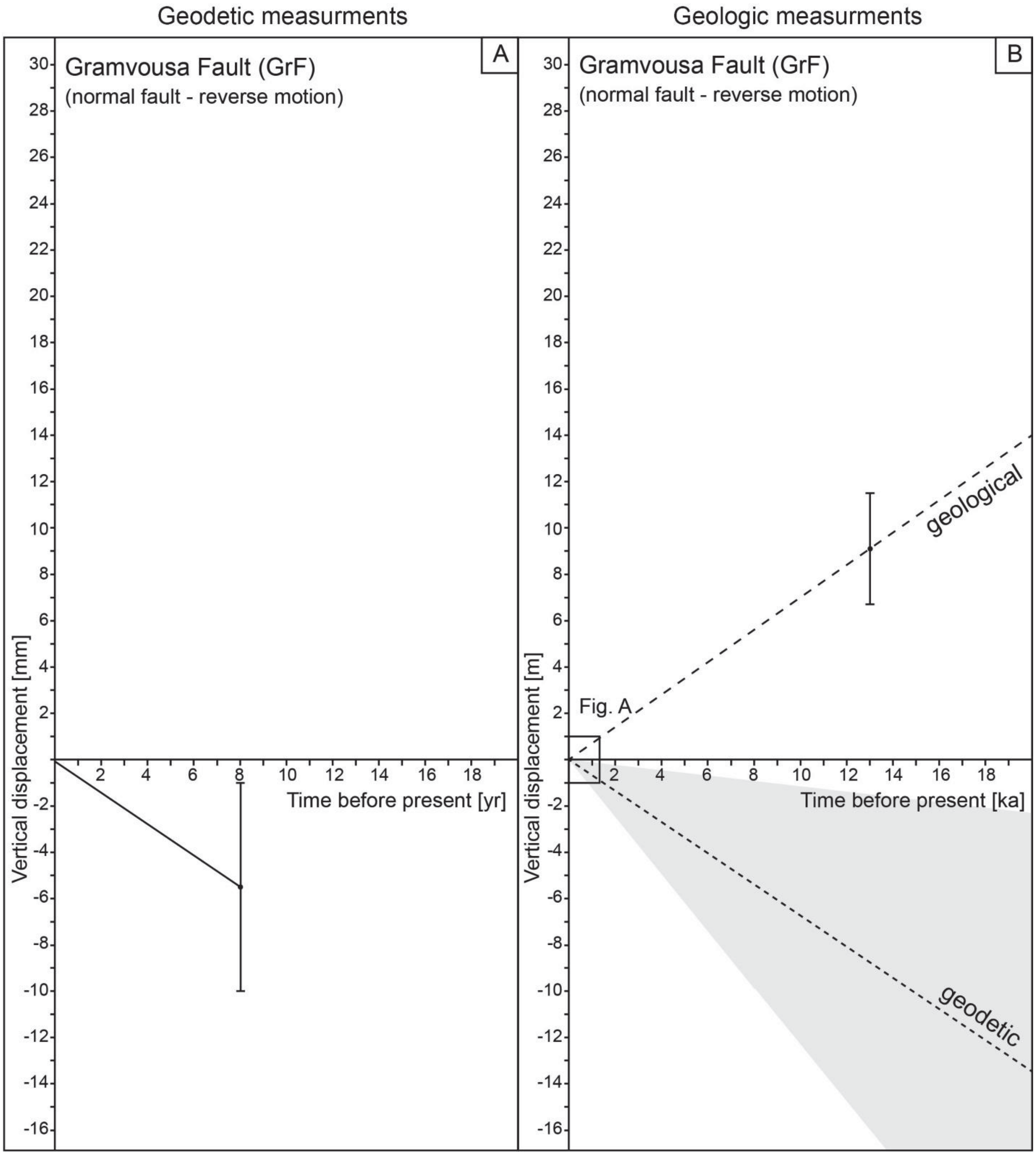

Figure II.11: A) Shows the vertical displacement in mm/yr measured by PSI along the Gramvousa fault. B) Shows the geodetic measurements versus the geologic slip-rate in ka/m derived from Caputo et al. (2010). The grey shade shows the error range of PSI measurements adjusted to the geological time.

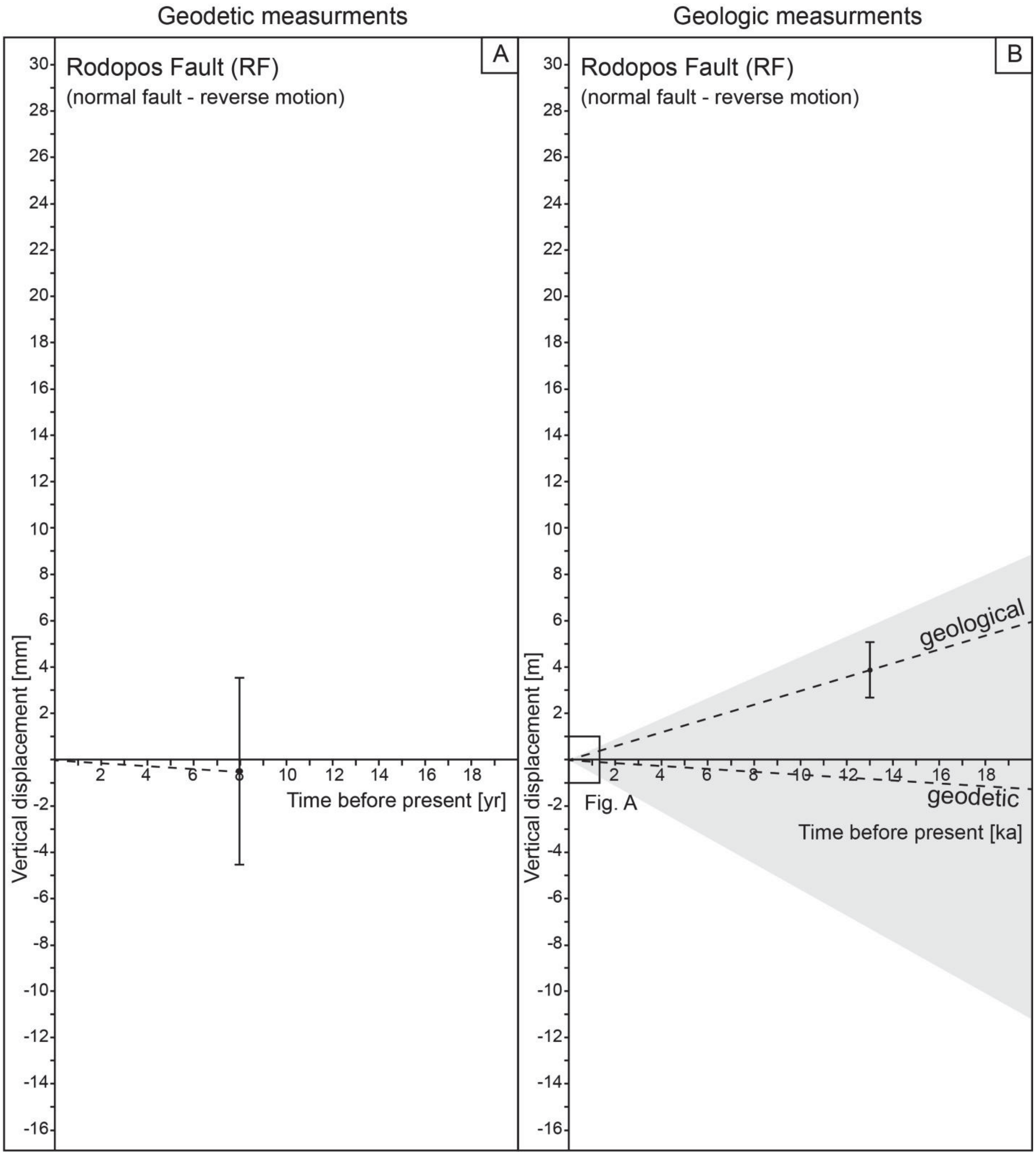

Figure II.12: A) Shows the vertical displacement in mm/yr measured by PSI along the Rodopos fault. B) Shows the geodetic measurements versus the geologic slip-rate in ka/m derived from Caputo et al. (2010). The grey shade shows the error range of PSI measurements adjusted to the geological time.

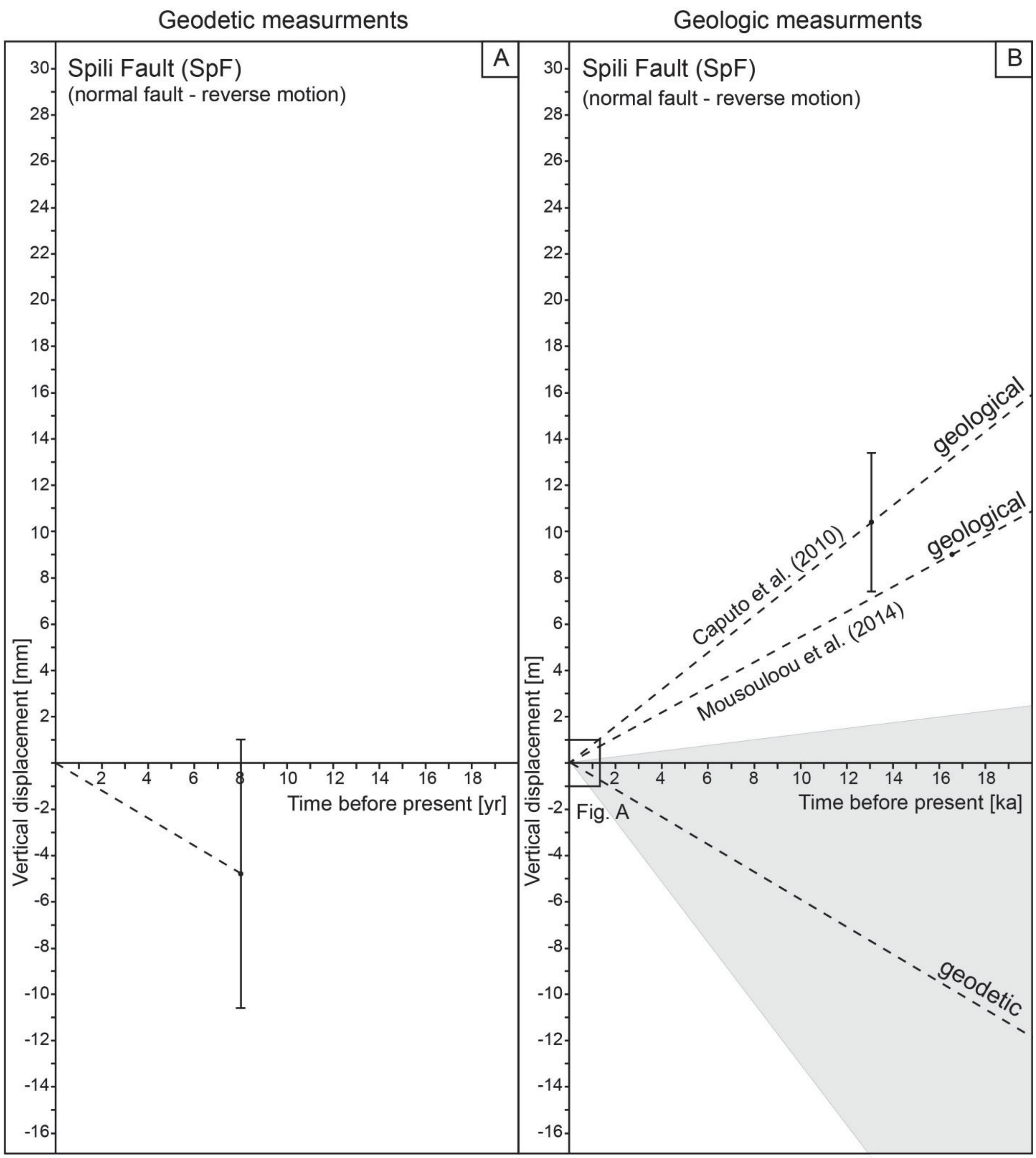

Figure II.13: A) Shows the vertical displacement in mm/yr measured by PSI along the Spili fault. B) Shows the geodetic measurements versus the geologic slip-rate in ka/m derived from Caputo et al. (2010). The grey shade shows the error range of PSI measurements adjusted to the geological time.

Chapter 4

II.1 Pleistocene and Holocene uplift rates based on paleo-shorelines

II.1.1 Ierapetra

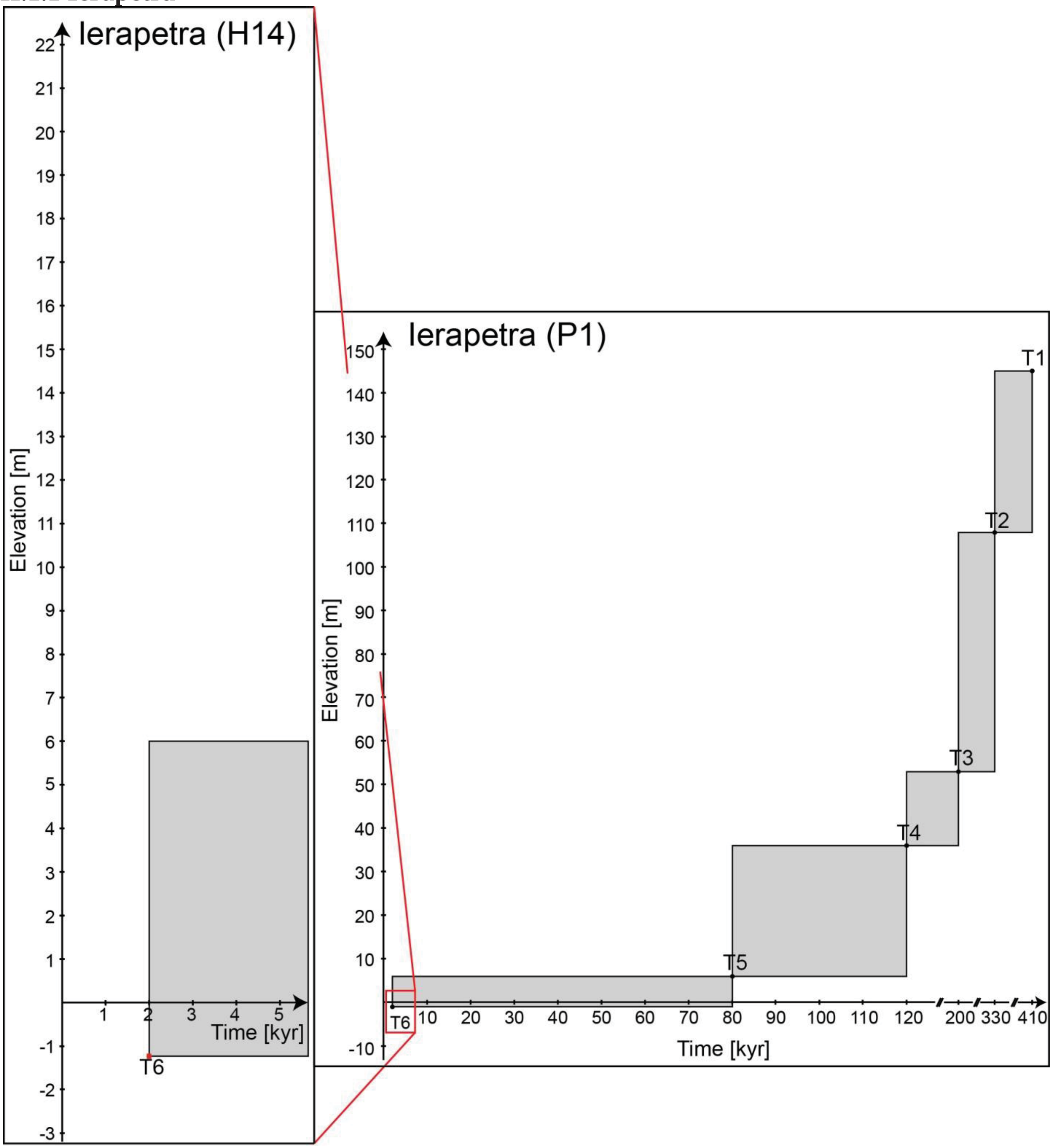

Figure II.14: Elevation of Pleistocene and Holocene paloe-shorelines plotted against time, modified after Gaki-Papanastassiou et al. (2009) and Mourtzas (2012).

II.1.1.1 Uplift rates only by tectonics

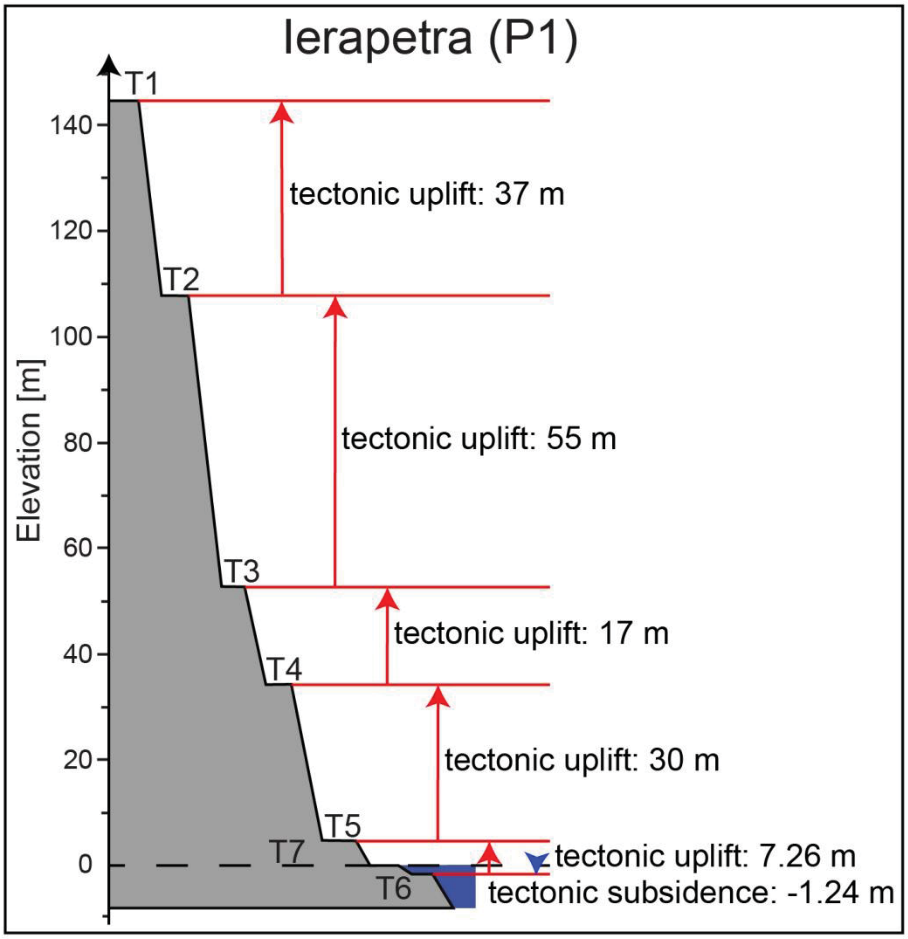

Figure II.15: Elevation of terraces and the height difference needed for the tectonic uplift, modified after Gaki-Papanastassiou et al. (2009) and Mourtzas (2012).

Table II.2: Terraces, their age, present elevation and calculated uplift rate. No sea-level.

Location	Terrace	Time *(T)* $[kyr]$	Elevation present *Ep* [m]	Uplift rate *(R)*[e] $[\frac{m}{kyr}]$
Ierapetra	T1[1]	404	145[c]	0.36
	T2[1]	327	108[c]	0.33
	T3[1]	197	53[c]	0.27
	T4[1]	120[a]	36[c]	0.3
	T5[1]	107	6[c]	0.06
	T6[2]	2[b]	-1.24[d]	-0.62

[1]Gaki-Papanastassiou et al. (2009); [2]Mourtzas (2012)
[a]Ages taken from my calculations and sea-level curve of Rohling et al. (2014).
[b]Ages taken from Mourtzas (2012).
[c]Present elevation taken from Gaki-Papanastassiou et al. (2009).
[d]Present elevation taken from Mourtzas (2012).
[e]Uplift rate calculated using equation: R = (Ep-E0) / T

Table II.3: Average uplift rate, slip rate, and recurrence time.

Average uplift rate (R) [mm/yr]	Slip rate [mm/yr]	Recurrence time [yr]
0.12	0.17	47058.8

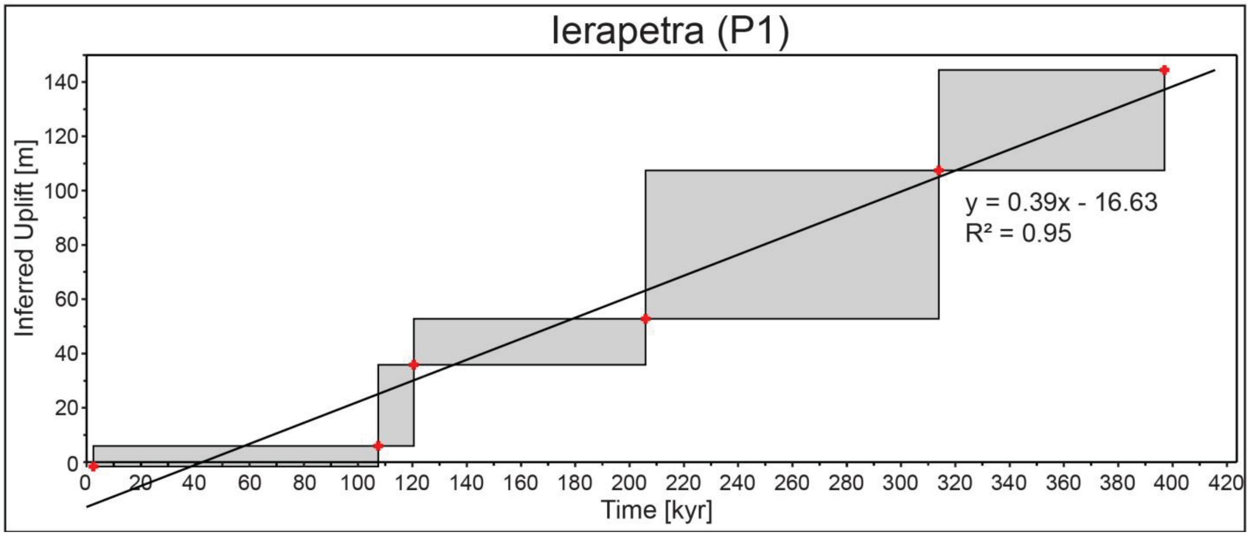

Figure II.16: Inferred uplift diagram curve for tectonic uplift is determined by linear regression analysis.

II.1.1.2 Uplift rates only by sea-level

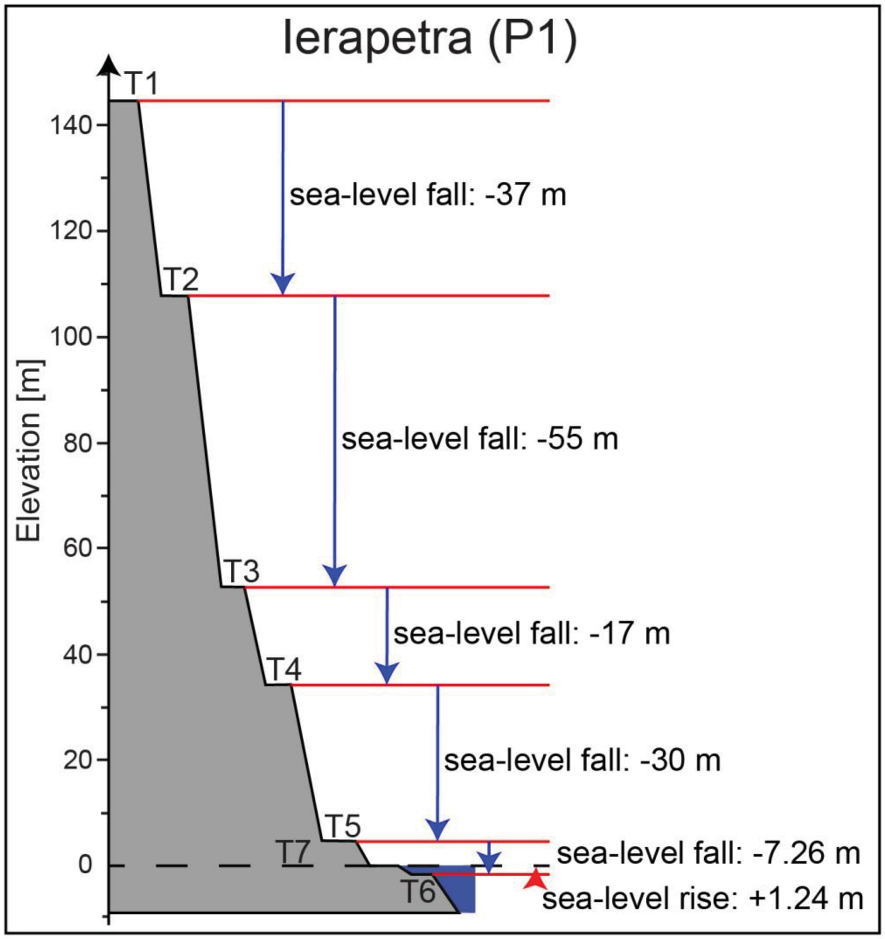

Figure II.17: Elevation of terraces and the needed amount of sea-level fall, modified after Gaki-Papanastassiou et al. (2009) and Mourtzas (2012).

Table II.4: Terraces, their age and calculated age, present elevation and sea-level change rate. No tectonics.

Location	**Terrace**	**Time *(T)* $[kyr]$**	**Elevation present *Ep* [m]**	**Sea-level change to lower terrace [m]**	**Sea-level change rate[h] $[\frac{m}{kyr}]$**
Ierapetra	T1[1]	404[a]	145[d]	-37[f]	0.09
	T2[1]	327[a]	108[d]	-55[f]	0.17
	T3[1]	197[a]	53[d]	-17[f]	0.08
	T4[1]	**120[b]**	**36[d]**	**-30[f]**	**0.25**
	T5[1]	107[a]	6[d]	-7.26[f]	0.07
	T6[2]	**2[c]**	**-1.24[e]**	+1.24[g]	0.62
Today shoreline	T7	0	0		

[1]Gaki-Papanastassiou et al. (2009); [2]Mourtzas (2012)
[a]Ages taken from my calculations and sea-level curve of Rohling et al. (2014).
[b]Ages taken from Gaki-Papanastassiou et al. (2009).
[c]Ages taken from Mourtzas (2012).
[d]Present elevation taken from Gaki-Papanastassiou et al. (2009).
[e]Present elevation taken from Mourtzas (2012).
[f]Sea-level fall → -
[g]Sea-level rise → +
[h]Sea-level change rate calculated using equation: sea-level change rate = (height change / age)

II.1.1.3 Constant uplift rates by tectonics and sea-level change

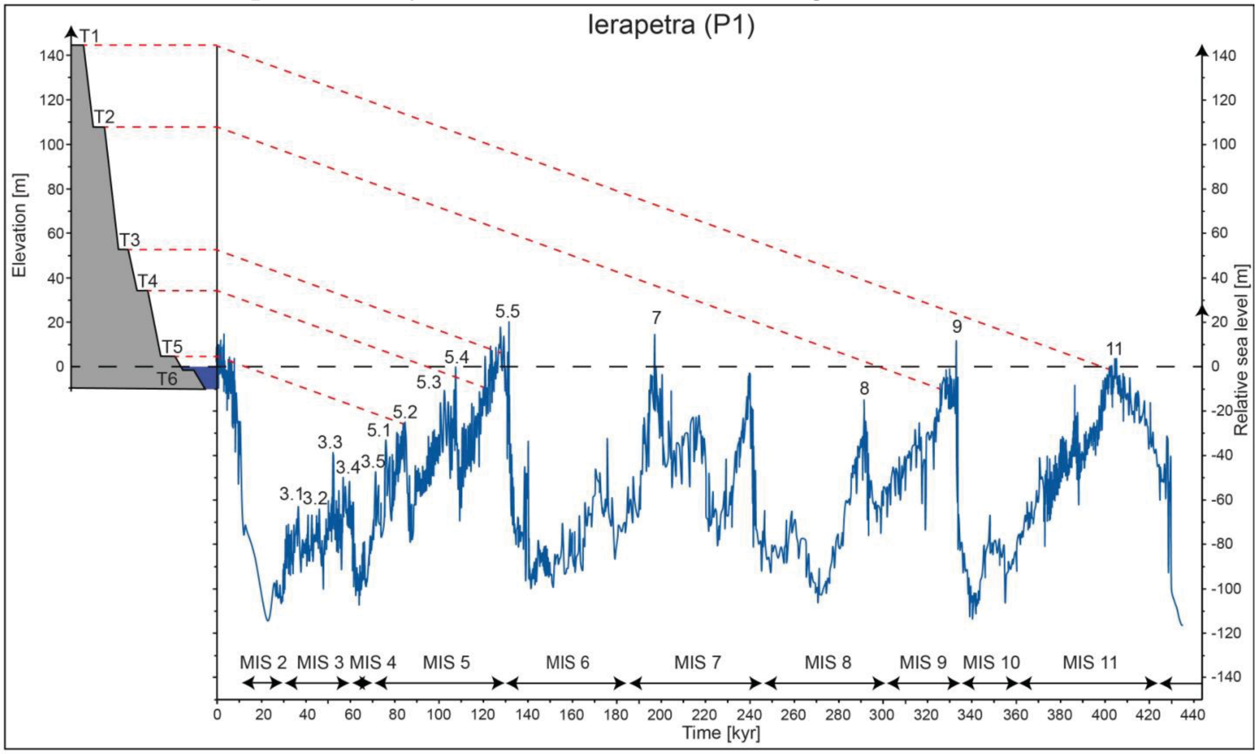

Figure II.18: Correlation of terraces at Ierapetra with the sea-level curve of Rohling et al. (2014), modified after Gaki-Papanastassiou et al. (2009) and Mourtzas (2012).

Table II.5: Ierapetra (P1) terrace numbers, elevation heights, and uplift rates (Rohling et al., 2014).

Location	Terrace	Time *(T)* $[kyr]$	Elevation present *Ep* [m]	Elevation original *E0* [m]	$E_p - E_o$ $[m]$	Uplift rate $(R)^f[\frac{m}{kyr}]$	Dated material
Ierapetra	T1[1]	401	145[c]	-1±6[e]	146±6	0.36±0.01	
	T2[1]	326	108[c]	-10±6[e]	118±6	0.36±0.02	
	T3[1]	128	53[c]	7±6[e]	46±6	0.36±0.03	
	T4[1]	**120[a]**	**36[c]**	-12.10±6[e]	48.10±6	0.40±0.05	*
	T5[1]	83	6[c]	-26±6[e]	32±6	0.38±0.06	
	T6[2]	**2[b]**	**-1.24[d]**	**0**	**-1.24**	**-0.62**	**

Bold terraces are dated terraces.
[1]Gaki-Papanastassiou et al. (2009); [2]Mourtzas (2012)
[a]Ages taken from Gaki-Papanastassiou et al. (2009).
[b]Ages taken from Mourtzas (2012).
[c]Present elevation taken from Gaki-Papanastassiou et al. (2009).
[d]Present elevation taken from Mourtzas (2012).
[e]Sea-level correction done after Rohling et al. (2014).
[f]Uplift rate calculated using equation: R = (Ep-E0) / T
*Radiometric dates and associated errors taken from Angelier (1979):
- Radiometric method $^{231}Pa/^{235}U$ dated fauna Pectenidae and Callista Chione at altitude 10 m with an age of 109^{+22}_{-12} ka and $130^{+\infty}_{-65}$, respectively
- Radiometric method $^{230}Th/^{235}U$ dated fauna Pectenidae at altitude 10 m with an age of 131^{+9}_{-7} and 103^{+6}_{-6}ka and $130^{+\infty}_{-65}$, and Callista Chione at altitude 10 m with an age of 90^{+5}_{-3} ka

**Mourtzas (2012)

Table II.6: Average uplift rate, slip rate, and recurrence time.

Average uplift rate (R) [mm/yr]	Slip rate [mm/yr]	Recurrence time [yr]
41 ± 0.03	0.83±0.04 mm/yr	9368 (+6666.67 / -4761.9)

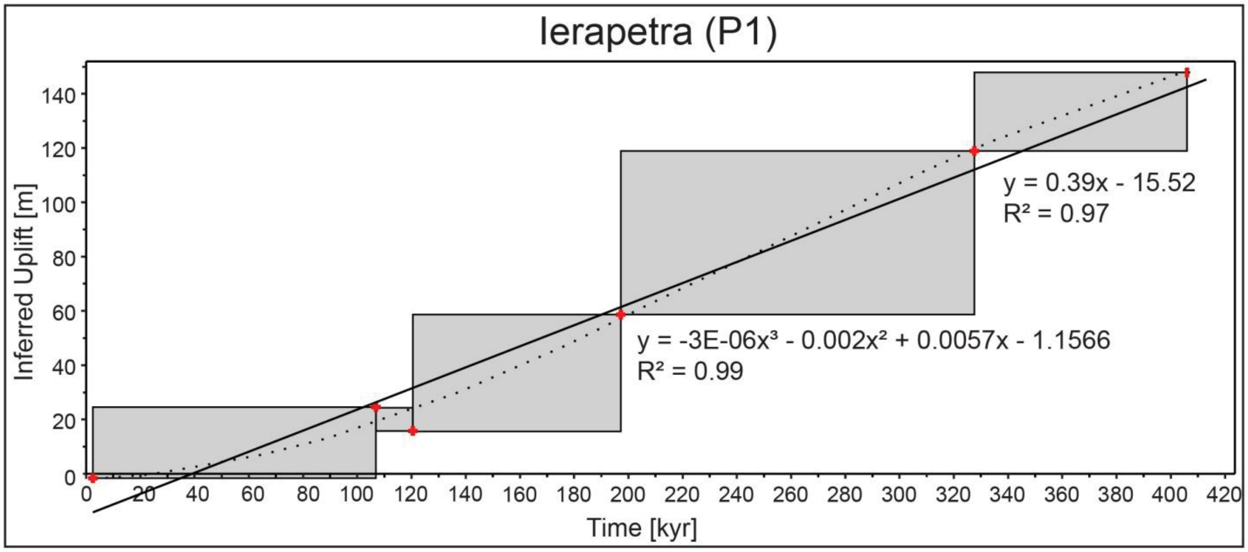

Figure II.19: Inferred uplift diagram curve for sea-level correction is determined by linear regression analysis.

II.1.2 Aradena Gorge

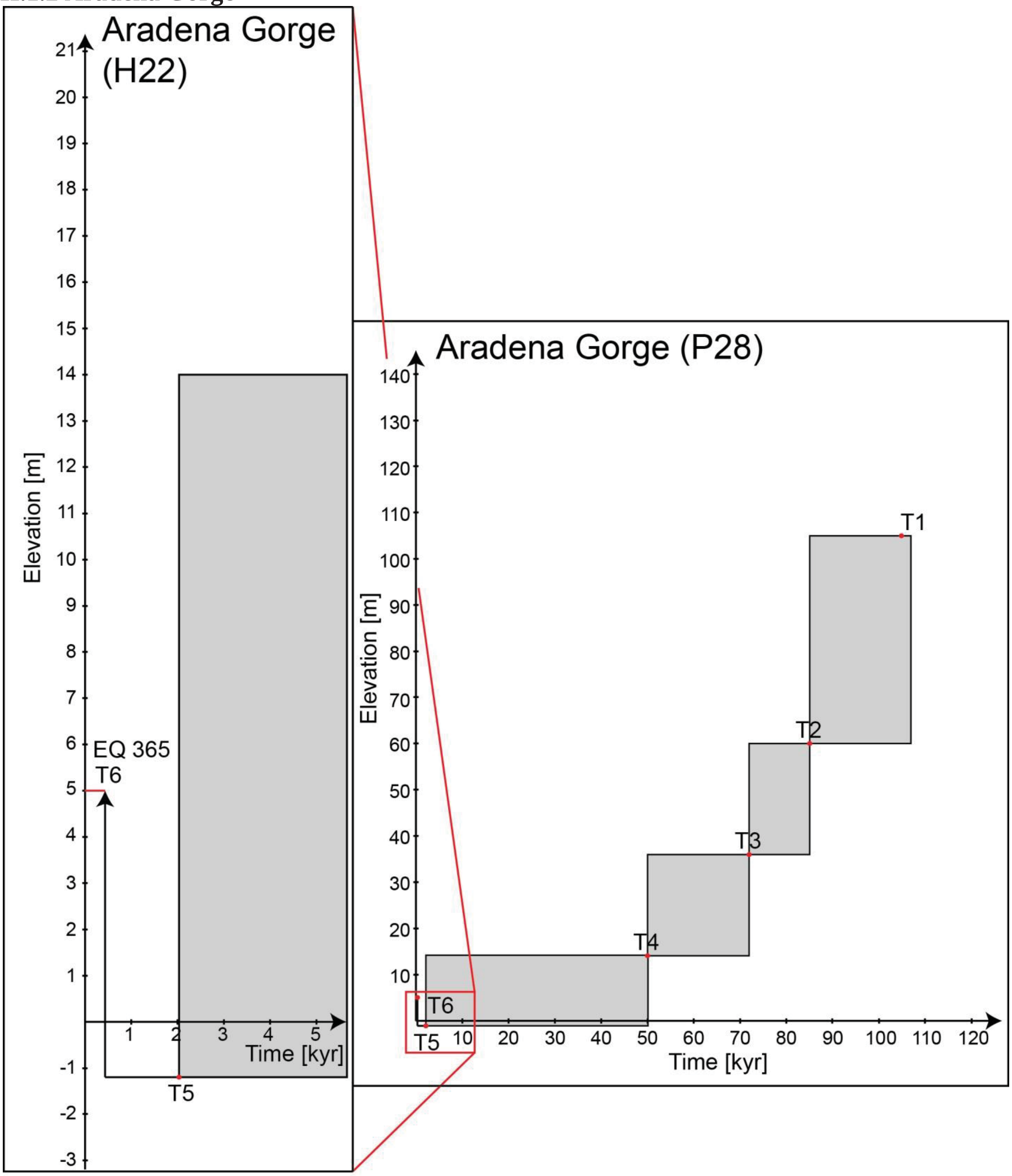

Figure II.20: Elevation of Pleistocene and Holocene paloe-shorelines plotted against time, modified after Wegmann (2008), Mourtzas (2012), and Pirazzoli et al. (1996). Elevation uncertainties for Pleistocene terraces are ± 1 m (Wegmann, 2008).

II.1.2.1 Uplift rates only by tectonics

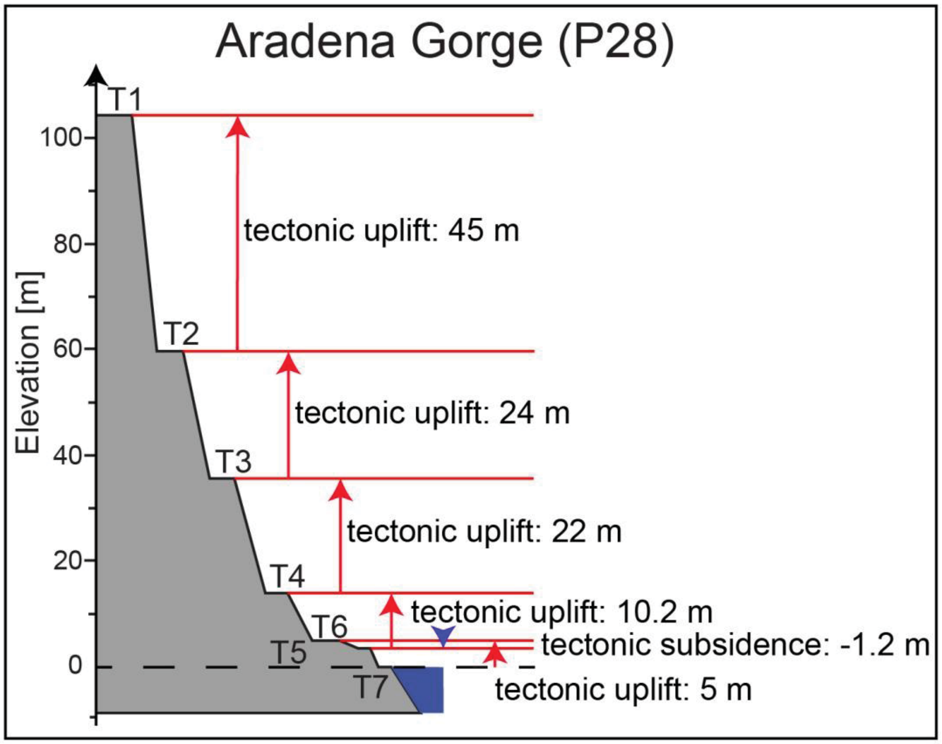

Figure II.21: Elevation of terraces and the height difference needed for the tectonic uplift, modified after Wegmann (2008), Mourtzas (2012), and Pirazzoli et al. (1996).

Table II.7: Terraces, their age, present elevation and calculated uplift rate. No sea-level.

Location	**Terrace**	**Time *(T)* $[kyr]$**	**Elevation present *Ep* [m]**	**Uplift rate *(R)*[g] $[\frac{m}{kyr}]$**
Aradena Gorge (P28 & H22)	T1[1]	107[a]	105[d]	0.98
	T2[1]	85[a]	60[d]	0.71
	T3[1]	72[a]	36[d]	0.50
	T4[1]	50[a]	14[d]	-0.28
	T5[2]	**2,05[b]**	**3,8[e]**	**1.85**
365 A.D. earthquake	**T6[3]**	**0.365[c]**	**5[f]**	**13.69**

[1]Wegmann (2008); [2]Mourtzas (2012); [3]Pirazzoli et al. (1996)
[a]Ages taken from Wegmann (2008).
[b]Ages taken from Mourtzas (2012).
[c]Ages taken from Pirazzoli et al. (1996).
[d]Present elevation taken from Wegmann (2008).
[e]Present elevation taken from Mourtzas (2012).
[f]Present elevation taken from Pirazzoli et al. (1996).
[g]Sea-level change rate calculated using equation: sea-level change rate = (height change / age)

Table II.8: Average uplift rate, slip rate, and recurrence time.

Average uplift rate (R) [mm/yr]	Slip rate [mm/yr]	Recurrence time [yr]
0.75	1.5	13333.33

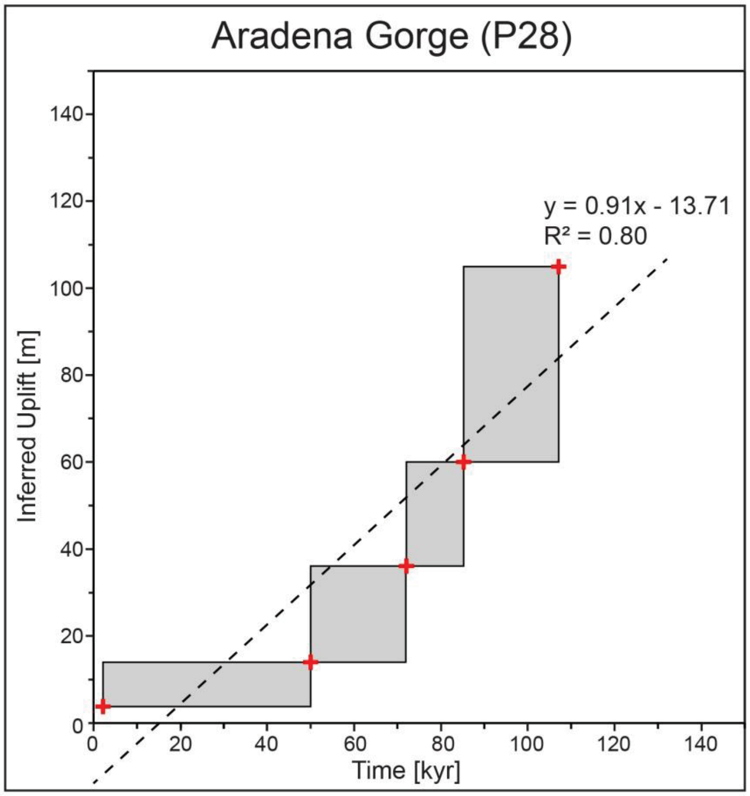

Figure II.22: Inferred uplift diagram curve for tectonic uplift is determined by linear regression analysis.

Table II.9: Displacement between terraces, the corresponding slip, M_0 and M_w.

Terraces	Terrace elevation [m]	Terrace elevation [m]	Displacement between terraces [m]	Correspnding slip along the Hellenic trench [m][a]	M_0[b] [dyne/cm]	M_w[c]
T6 – T5	T6 = 5	T5 = 3.8	~1.0	20	$2.7*10^{28}$	8.25
T5 – T4	T5 = 3.8	T4 = 14	~10.0	200	$2.7*10^{29}$	8.29
T4 – T3	T4 = 14	T3 = 36	22	440	$5.9*10^{29}$	9.14
T3 – T2	T3 = 36	T2 = 60	24	480	$6.48*10^{29}$	9.17
T2 – T1	T2 = 60	T1 = 105	45	900	$1.21*10^{30}$	9.35

[a]Corresponding slip along is measured based on the slip of 20 m which equals a vertical displacement of 9 m

[b]Seismic Moment: $M_0 = \mu AD$

[c]Moment Magnitude: $M_w = \frac{2}{3} log M_0 - 10.7$

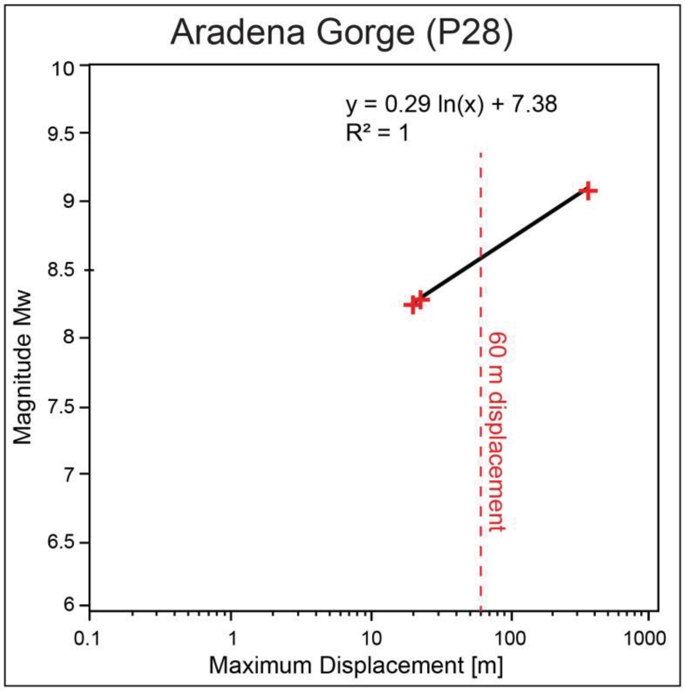

Figure II.23: Regression of maximum displacement versus magnitude Mw. Maximum displacement 60 m ever measured for an earthquake is for the 2011 Mw 9.0 Tohoku-Oki (Japan).

For the 2011 Mw 9.0 Tohoku-Oki (Japan) earthquake the maximum slip is modeled with displacement of around 60 m (Simons et al., 2011). For the 2010 Mw 8.8 Maule (Chile) earthquake the maximum slip reached around 15 m (Vigny et al., 2011). The maximum slip of 15 m was modeled for the 2004 Mw 9.1 Sumatra-Andaman earthquake (Ammon et al., 2005). For the 1960 Mw 9.5 Chile earthquake the maximum slip is on the order of 17 m for a uniform slip planar model, and for a variable slip planar model, representing slip along asperities, the highest peak of slip reached a value of 41 m (Barrientos and Ward, 1990).

II.1.2.2 Uplift rates only by sea-level changes

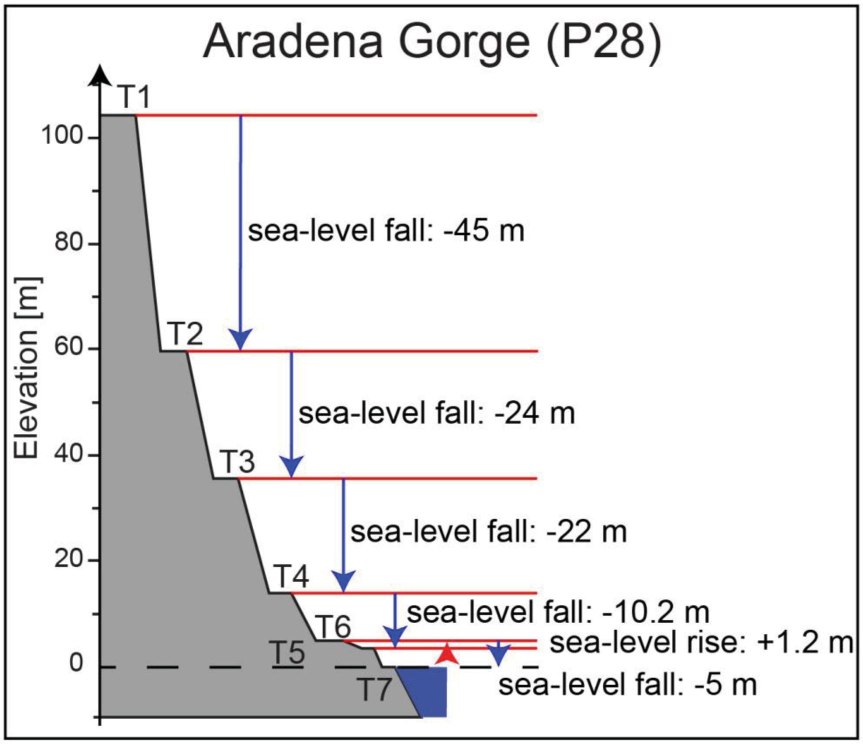

Figure II.24: Elevation of terraces and the needed amount of sea-level fall, modified after Wegmann (2008), Mourtzas (2012), and Pirazzoli et al. (1996).

Table II.10: Terraces, their age and calculated age, present elevation and sea-level change rate. No tectonics.

Location	**Terrace**	**Time *(T)*** $[kyr]$	**Elevation present *Ep* [m]**	**Sea-level change to lower terrace [m]**	**Sea-level change rate[i]** $[\frac{m}{kyr}]$
Aradena Gorge (P28 & H22)	T1[1]	107.9[a]	105[d]	-45[g]	0.42
	T2[1]	84.8[a]	60[d]	-24[g]	0.28
	T3[1]	71.8[a]	36[d]	-22[g]	0.31
	T4[1]	52.5[a]	14[d]	-10.2[g]	0.19
	T5[2]	**2.05[b]**	**3.8[e]**	**+1.2[h]**	0.58
365 A.D. earthquake	**T6[3]**	**0.365[c]**	**5[f]**	**-5[g]**	**-13.69**
Today shoreline	**T7**	**0**	**0**		

[1]Wegmann (2008); [2]Mourtzas (2012); [3]Pirazzoli et al. (1996)
[a]Ages taken from Wegmann (2008). MIS stages taken and ages corrected after Rohling et al. (2014).
[b]Ages taken from Mourtzas (2012).
[c]Ages taken from Pirazzoli et al. (1996).
[d]Present elevation taken from Wegmann (2008).
[e]Present elevation taken from Mourtzas (2012).
[f]Present elevation taken from Pirazzoli et al. (1996).
[g]Sea-level fall → -
[h]Sea-level rise → +
[i]Sea-level change rate calculated using equation: sea-level change rate = (height change / age)

II.1.2.3 Uplift rates by tectonics and sea-level change

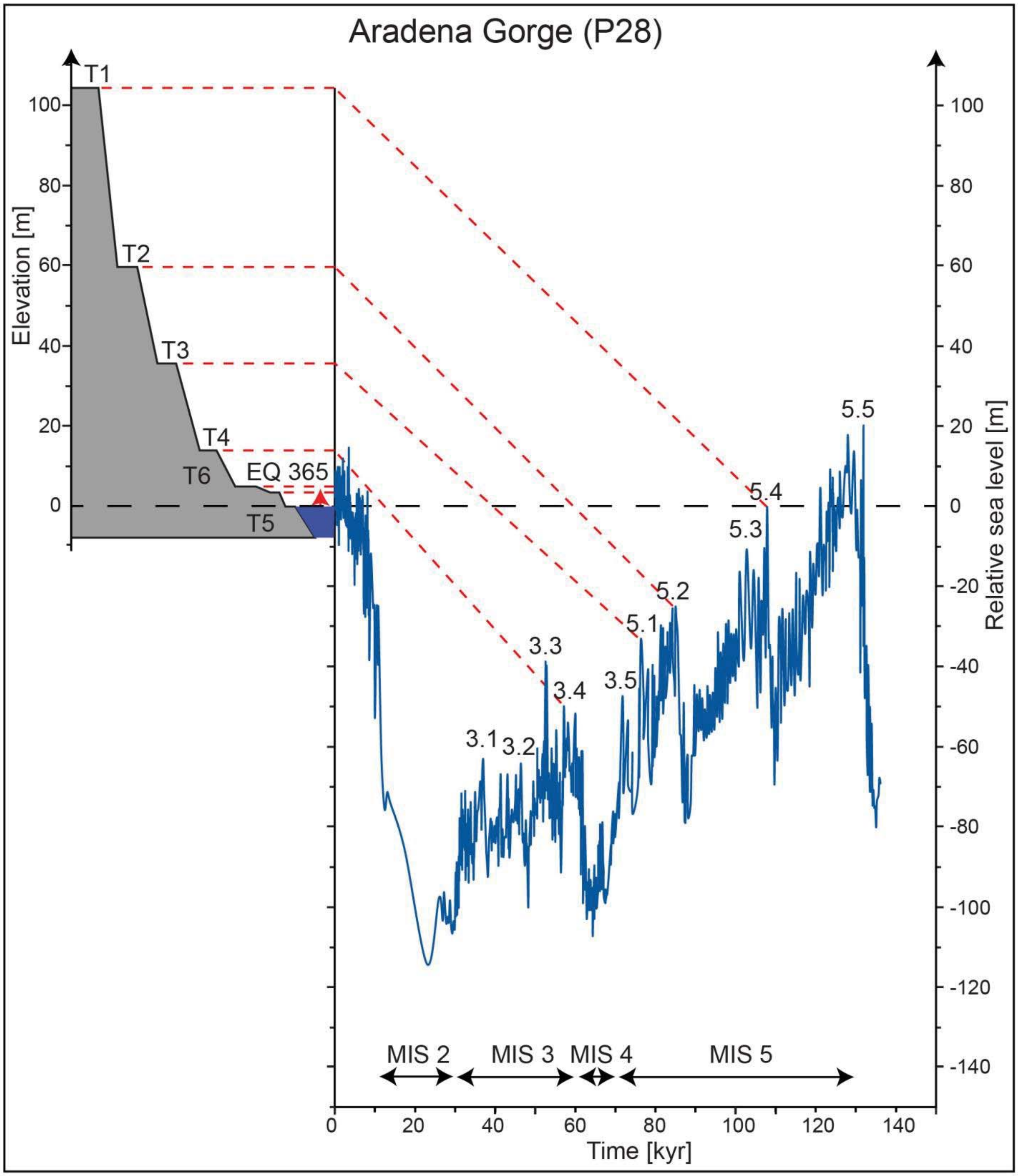

Figure II.25: Correlation of terraces at Aradena Gorge with the sea-level curve of Rohling et al. (2014), modified after Wegmann (2008), Mourtzas (2012), and Pirazzoli et al. (1996).

Table II.11: Terrace numbers, elevation heights, and uplift rates. Sea-level corrected and tectonics (Rohling et al., 2014).

Location	Terrace	Time *(T)* $[kyr]$	Elevation present *Ep* [m]	Elevation original *E0* [m]	$E_p - E_o$ $[m]$	Uplift rate *(R)*[h] $[\frac{m}{kyr}]$	Dated material
Aradena Gorge (P28 & H22)	T1[1]	107.9[a]	105±1[d]	-19.50±6[g]	124.5±6.08	1.15±0.06	*
	T2[1]	84.8[a]	60±1[d]	-47.1±6[g]	107.1±6.08	1.26±0.07	*
	T3[1]	71.8[a]	36±1[d]	-53.3±6[g]	89.3±6.08	1.24±0.08	*
	T4[1]	52.5[a]	14±1[d]	-55.8±6[g]	69.8±6.08	1.33±0.12	**
	T5[2]	**2.05[b]**	**3.8[e]**	**0**	**3.8**	**1.85**	***
365 A.D. earthquake	**T6[3]**	**0.365[c]**	**5[f]**	**0**	**5**	**13.69**	

Bold terraces are dated terraces.
[1]Wegmann (2008); [2]Mourtzas (2012); Pirazzoli et al. (1996)
[a]Ages taken from Wegmann (2008). MIS stages taken and ages corrected after Rohling et al. (2014).
[b]Ages taken from Mourtzas (2012).
[c]Ages taken from Pirazzoli et al. (1996).
[d]Present elevation taken from Wegmann (2008).
[e]Present elevation taken from Mourtzas (2012).
[f]Present elevation taken from Pirazzoli et al. (1996).
[g]Sea-level correction done after Rohling et al. (2014).
[h]Uplift rate calculated using equation: R = (Ep-E0) / T
*Facies relationship for lateral correlation of spatially separated locations are taken from Wegmann (2008): Facies D - Corresponds to clastic pebble-to cobble beach associated with wave-cut erosion notch.
** Facies relationship for lateral correlation of spatially separated locations are taken from Wegmann (2008): Facies A - Corresponds to Algal bioherms and patch reefs along sediment-poor coastline
***Mourtzas (2012)

Table II.12: Average uplift rate, slip rate, and recurrence time.

Average uplift rate (R) [mm/yr]	Slip rate [mm/yr]	Recurrence time [yr]
1.37 ± 0.08	2.74 ± 0.16	7299.27 (+452.67 / -402.72)

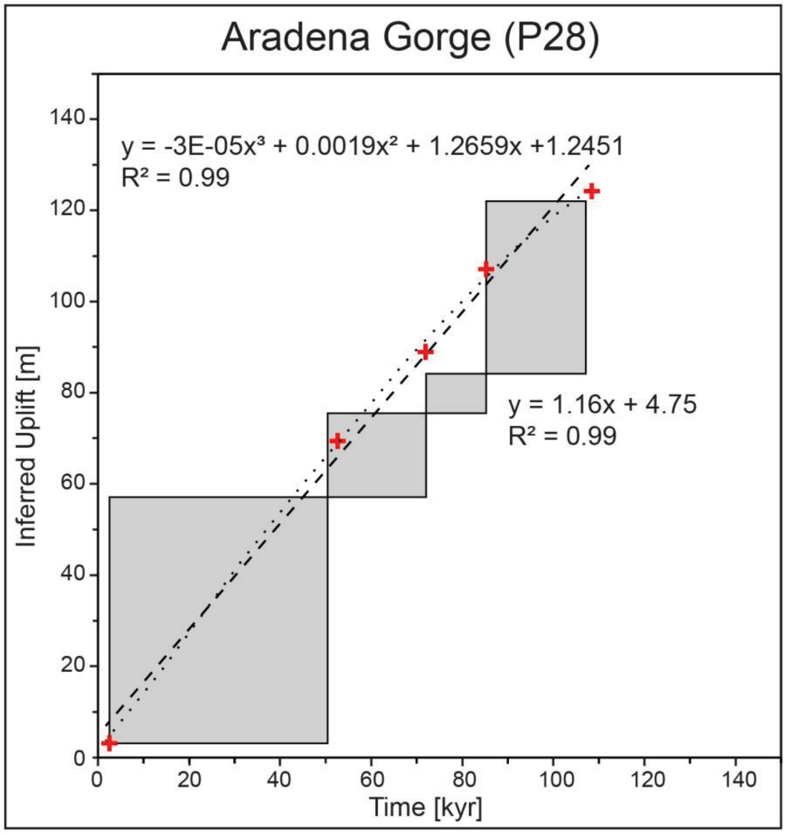

Figure II.26: Inferred uplift diagram curve for tectonic uplift is determined by linear regression analysis.

Table II.13: Average uplift rate, slip rate, recurrence time for the 21st July 365 A.D. earthquake, and total slip for highest and oldest terrace at Aradena Gorge.

Earthquake 21st July 365 A.D.	Mw	Time interval [kyr]	Average uplift rate [mm/yr]	Slip rate [mm/yr]	Recurrence time [yr]	Total slip for highest and oldest terrace [m]
Aradena Gorge Tectonic only	8.25[1]	107[2] until today	0.75	1.5	13333.33	160.5
Aradena Gorge Sea-level corrected[3]	8.25[1]	107[2] until today	1.37±0.08	2.74±0.16	7299.27	295.65

[1] Shaw et al. (2008); [2]Wegmann (2008); [3]Rohling et al. (2014)

II.1.3 Sougia

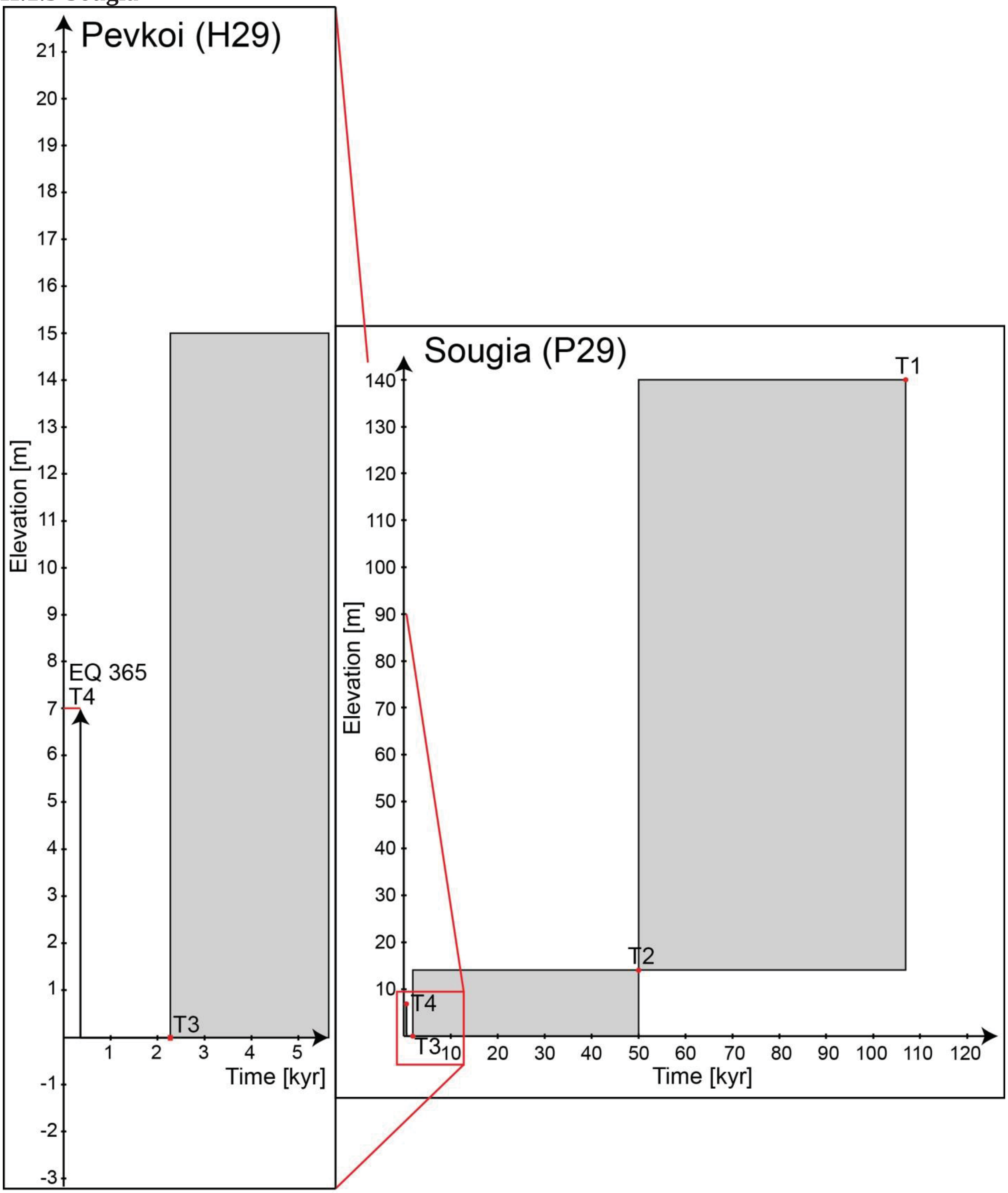

Figure II.27: Elevation of Pleistocene and Holocene paloe-shorelines plotted against time, modified after Wegmann (2008), Pirazzoli et al. (1996), and Price et al. (2002). Elevation uncertainties for Pleistocene terraces are ± 1 m (Wegmann, 2008).

II.1.3.1 Uplift rates only by tectonics

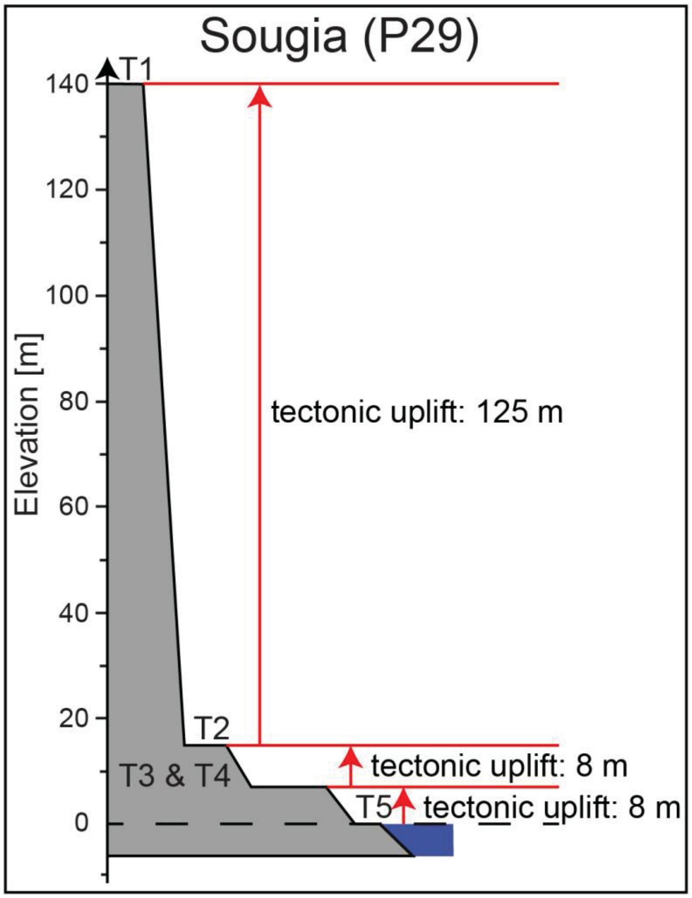

Figure II.28: Elevation of terraces and the height difference needed for the tectonic uplift, modified after Wegmann (2008), Pirazzoli et al. (1996), and Price et al. (2002).

Table II.14: Terraces, their age, present elevation and calculated uplift rate. No sea-level.

Location	Terrace	Time *(T)* $[kyr]$	Elevation present *Ep* [m]	Uplift rate *(R)*[h] $[\frac{m}{kyr}]$
Sougia (P29 & H29)	T1[1]	107[a]	140[e]	1.31
	T2[1]	50[a]	15[e]	0.30
Pevkoi	**T3[2]**	**2.250 ± 0.07[b]**	**7[f]**	**3.1±0.23**
	T3[3]	**2.280 ± 0.073[c]**	**7[g]**	**3.1±0.23**
365 A.D. earthquake	**T4[2]**	**0.365[b]**	**7[f]**	**19.18**

[1]Wegmann (2008); [2]Pirazzoli et al. (1996); [3]Price et al. (2002).
[a]Ages taken from Wegmann (2008).
[b]Ages taken from Pirazzoli et al. (1996).
[c]Ages taken from Price et al. (2002).
[e]Present elevation taken from Wegmann (2008).
[f]Present elevation taken from Pirazzoli et al. (1996).
[g]Present elevation taken from Price et al. (2002).
[h]Uplift rate calculated using equation: R = (Ep-E0) / T

Table II.15: Average uplift rate, slip rate, and recurrence time.

Average uplift rate (R) [mm/yr]	Slip rate [mm/yr]	Recurrence time [yr]
1.95 ± 0.23	3.9 ± 0.46	5128.21 (+685.74 / -541.05)

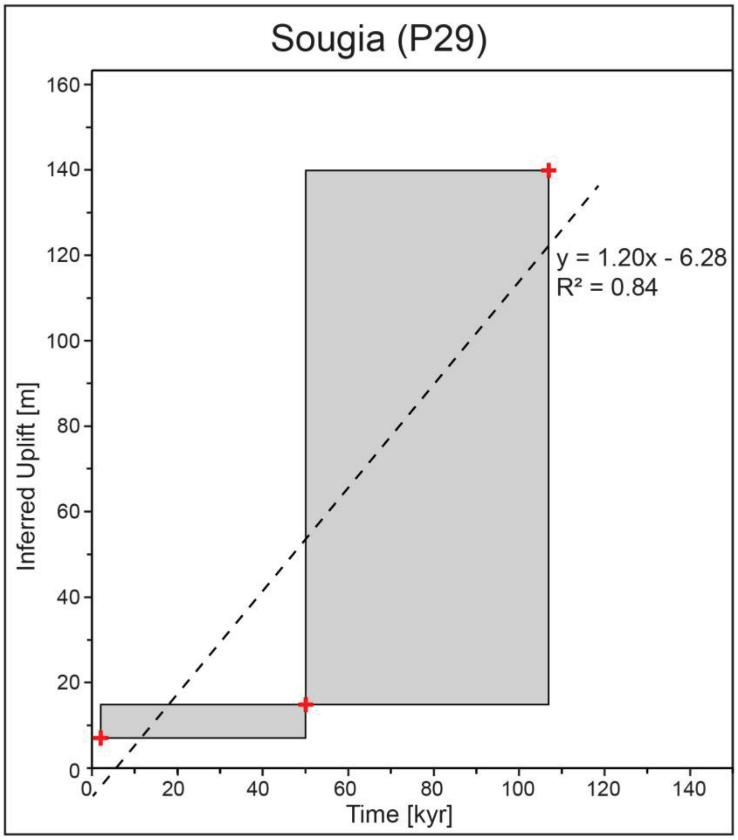

Figure II.29: Inferred uplift diagram curve for tectonic uplift is determined by linear regression analysis.

Table II.16: Displacement between terraces, the corrspnding slip, M_0 and M_w.

Terraces	Terrace elevation [m]	Terrace elevation [m]	Displacement between terraces [m]	Correspnding slip along the Hellenic trench [m][a]	M_0[b] [dyne/cm]	M_w[c]
T4 – T3	T4 = 7	T3 = 7	0	0	0	0
T3 – T2	T3 = 7	T2 = 15	8	22.86	$3.09*10^{28}$	8.29
T2 – T1	T2 = 15	T1 = 140	125	357.12	$4.82*10^{29}$	9.09

[a]Corresponding slip along is measured based on the slip of 20 m which equals a vertical displacement of 9 m

[b]Seismic Moment: $M_0 = \mu AD$

[c]Moment Magnitude: $M_w = \frac{2}{3} log M_0 - 10.7$

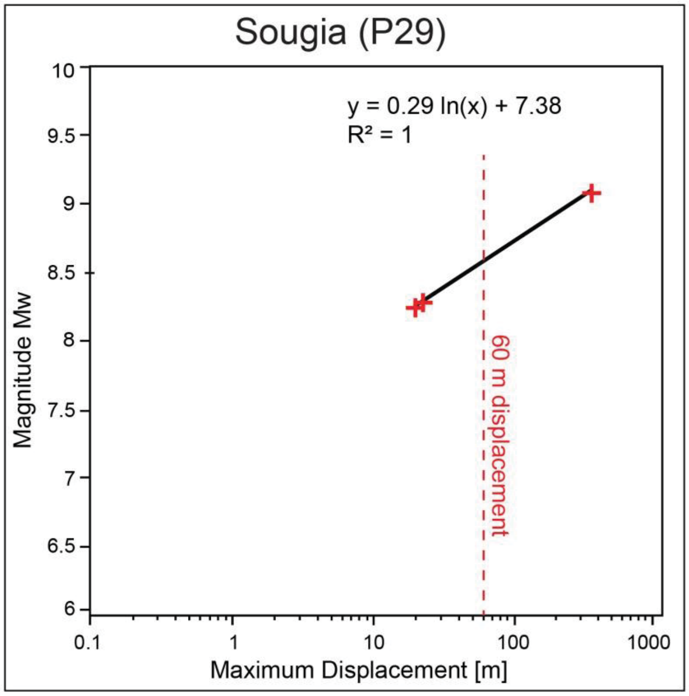

Figure II.30: Regression of maximum displacement versus magnitude Mw. Maximum displacement 60 m ever measured for an earthquake is for the 2011 Mw 9.0 Tohoku-Oki (Japan).

II.1.3.2 Uplift rates only by sea-level changes

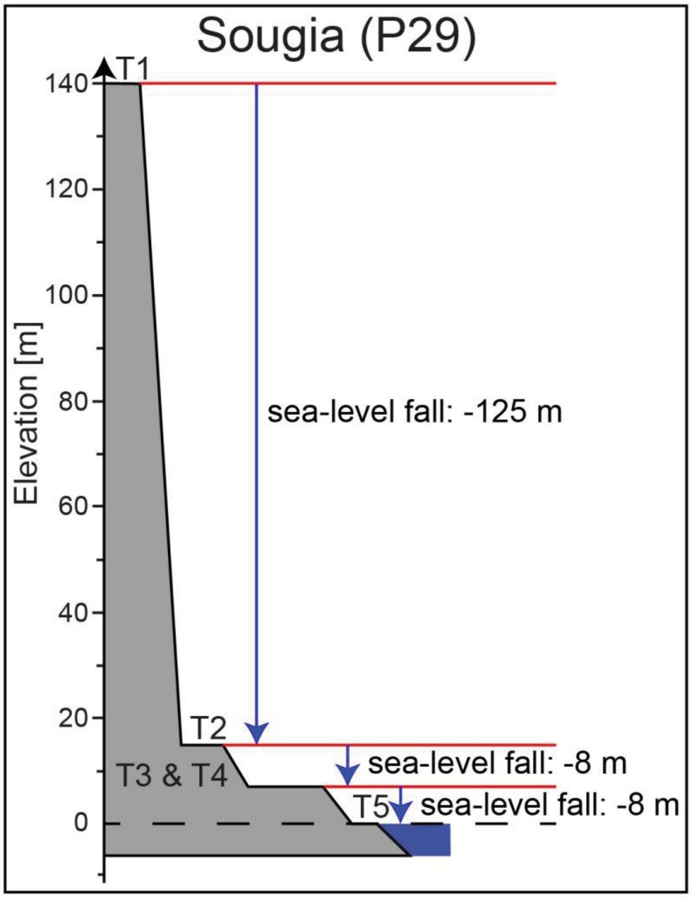

Figure II.31: Elevation of terraces and the needed amount of sea-level fall, modified after Wegmann (2008), Pirazzoli et al. (1996), and Price et al. (2002).

Table II.17: Terraces, their age and calculated age, present elevation and sea-level change rate. No tectonics.

Location	**Terrace**	**Time *(T)*** $[kyr]$	**Elevation present *Ep* [m]**	**Sea-level change to lower terrace [m]**	**Sea-level change rate[h]** $[\frac{m}{kyr}]$
Sougia (P29 & H29)	T1[1]	107.9[a]	140[d]	-125[g]	1.16
	T2[1]	52.9[a]	15[d]	-8[g]	0.15
Pevkoi	**T3[2]**	**2.250 ± 0.07[b]**	**7[e]**	0	0
	T3[3]	**2.280 ± 0.073[c]**	**7[f]**	0	0
365 A.D. earthquake	**T4[2]**	**0.365[b]**	**7[e]**	**-7[g]**	**19.18**
Today shoreline	**T5**	**0**	**0**		

[1]Wegmann (2008); [2]Pirazzoli et al. (1996); [3]Price et al. (2002).
[a]Ages taken from Wegmann (2008). MIS ages taken and than converted to ages with Rohling et al. (2014)
[b]Ages taken from Pirazzoli et al. (1996).
[c]Ages taken from Price et al. (2002).
[d]Present elevation taken from Wegmann (2008).
[e]Present elevation taken from Pirazzoli et al. (1996).
[f]Present elevation taken from Price et al. (2002).
[g]Sea-level fall → -
[h]Sea-level change rate calculated using equation: sea-level change rate = (height change / age)

II.1.3.3 Uplift rates by tectonic and sea-level changes

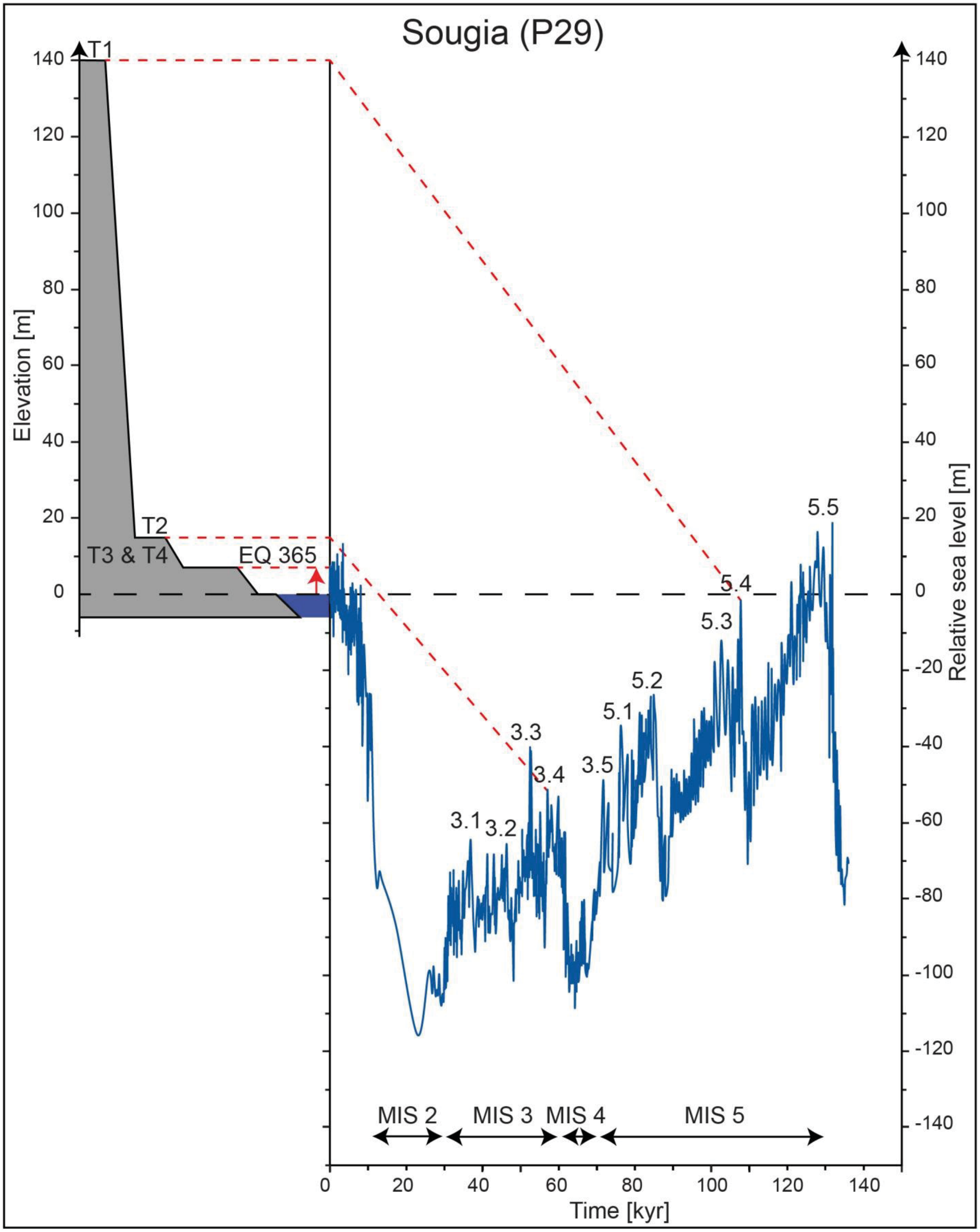

Figure II.32: Correlation of terraces at Sougia with the sea-level curve of Rohling et al. (2014), modified after Wegmann (2008), Pirazzoli et al. (1996), and Price et al. (2002).

Table II.18: Sougia terrace numbers, elevation heights, and uplift rates (Rohling et al., 2014).

Location	Terrace	Time *(T)* $[kyr]$	Elevation present *Ep* [m]	Elevation original *E0* [m]	$E_p - E_o$ $[m]$	Uplift rate *(R)*[i] $[\frac{m}{kyr}]$	Dated material
Sougia (P29 & H29)	T1[1]	107.9[a]	140±1[e]	-19.50±6[h]	159±6.08	1.48±0.06	*
	T2[1]	52.9[a]	15±1[e]	-55.8±6[h]	70.8±6.08	1.35±0.12	*
Pevkoi	**T3[2]**	**2.250 ± 0.07[b]**	**7[f]**	**0**	**7 ± 0.3**	**3.1 ± 0.23**	**
	T3[3]	**2.280 ± 0.073[c]**	**7[g]**	**0**	**7 ± 0.3**	**3.1 ± 0.23**	***
365 A.D. earthquake	**T4[2]**	**0.365[b]**	**7[f]**	**0**	**7**	**19.18**	

Bold terraces are dated terraces.
[1]Wegmann (2008); [2]Pirazzoli et al. (1996); [3]Price et al. (2002).
[a]Ages taken from Wegmann (2008). MIS ages taken and than converted to ages with Rohling et al. (2014)
[b]Ages taken from Pirazzoli et al. (1996).
[c]Ages taken from Price et al. (2002).
[e]Present elevation taken from Wegmann (2008).
[f]Present elevation taken from Pirazzoli et al. (1996).
[g]Present elevation taken from Price et al. (2002).
[h]Sea-level correction done after Rohling et al. (2014).
[i]Uplift rate calculated using equation: R = (Ep-E0) / T
*Facies relationship for lateral correlation of spatially separated locations are taken from Wegmann (2008): Facies D - Corresponds to clastic pebble-to cobble beach associated with wave-cut erosion notch.
**Radiocarbon date ^{14}C of Dendropoma (Novastoa) petraeum by Pirazzoli et al (1996). Calculated using a reservoir effect of 320 ± 25 years for the Mediterranean.
*** Radiocarbon date ^{14}C of Dendropoma by Price et al (2002). Corrected the original radiocarbon dates (BP) by adding 430 ^{14}C years to each.

Table II.19: Average uplift rate, slip rate, and recurrence time.

Average uplift rate (R) [mm/yr]	Slip rate [mm/yr]	Recurrence time [yr]
2.26 ± 0.16	4.52 ± 0.32	4424.78 (+337.12 / -292.55)

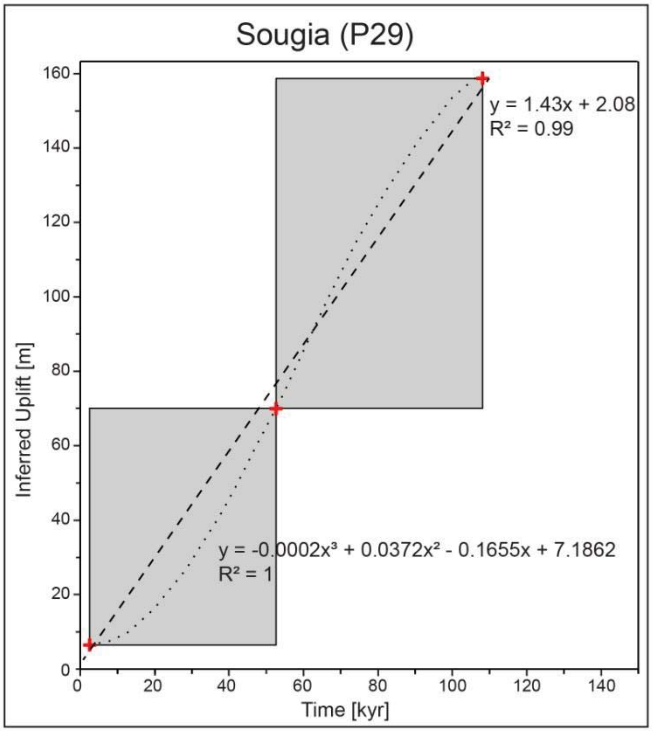

Figure II.33: Inferred uplift diagram curve for sea-level correction is determined by linear regression analysis.

Table II.20: Average uplift rate, slip rate, recurrence time for the 21st July 365 A.D. earthquake, and total slip for highest and oldest terrace at Sougia.

Earthquake 21st July 365 A.D.	Mw	Time interval [kyr]	Average uplift rate [mm/yr]	Slip rate [mm/yr]	Recurrence time [yr]	Total slip for highest and oldest terrace [m]
Sougia Tectonic only	8.25[1]	107[2] until today	1.95	3.9	5128.21	417.3
Sougia Constant Sea-level corrected[3]	8.25[1]	107[2] until today	2.26±0.16	4.52±0.32	4424.78	487.71

[1] Shaw et al. (2008); [2]Wegmann (2008); [3]Rohling et al. (2014)

II.1.4 Kalamia

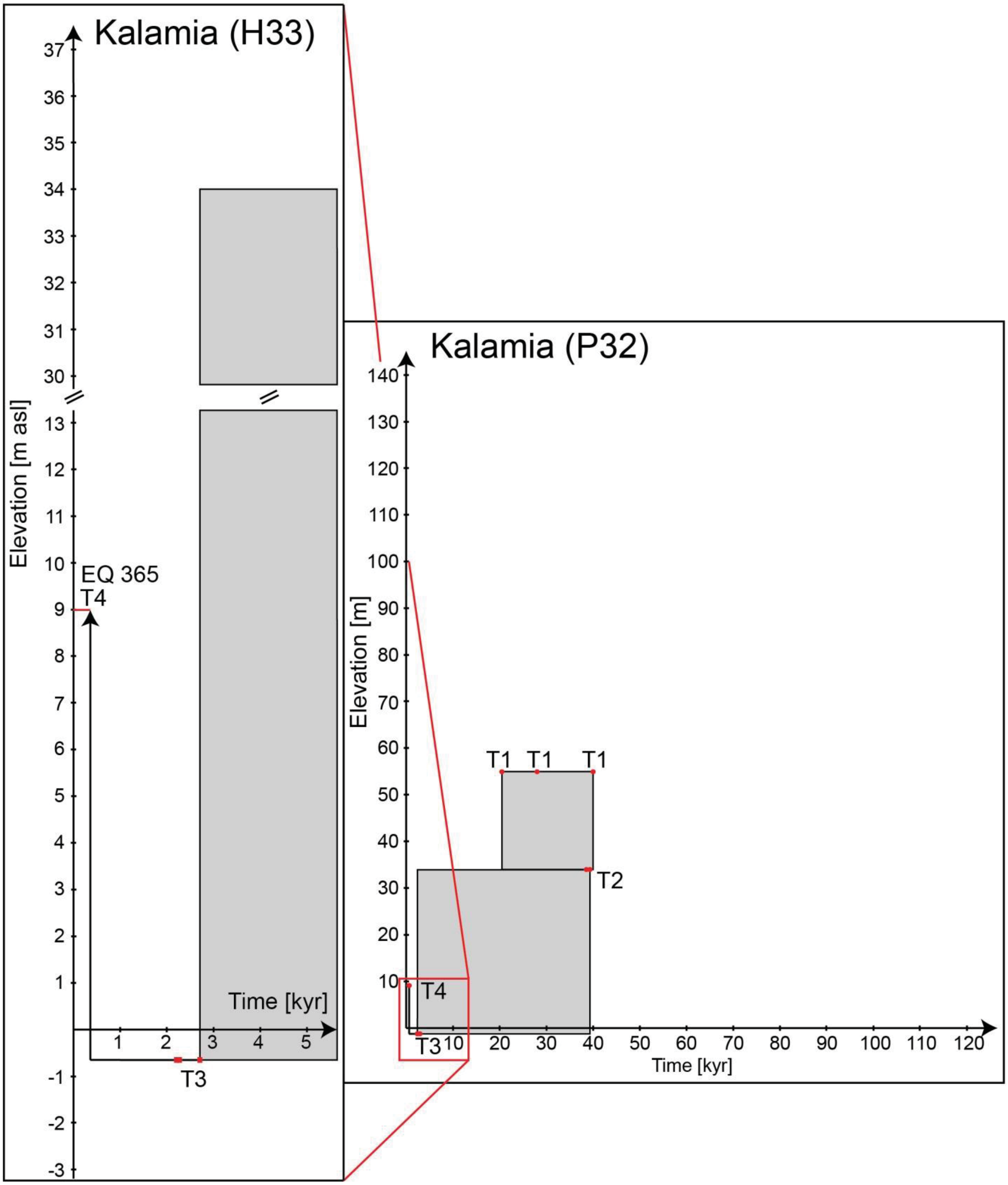

Figure II.34: Elevation of Pleistocene and Holocene paloe-shorelines plotted against time, modified after Tibert et al. (2014), and Pirazzoli et al. (1996).

II.1.4.1 Uplift rates only by tectonics

Table II.21: Terraces, their age, present elevation and calculated uplift rate. No sea-level.

Location	Terrace	Time *(T)* $[kyr]$	Elevation present *Ep* [m]	Uplift rate *(R)*[e] $[\frac{m}{kyr}]$
Kalamia (P32 & H33)	T1[1]	26.93 ± 0.0002[a]	55[c]	2.04
		19.48 ± 0.00009[a]	55[c]	2.82
		39.19 ± 0.0004[a]	55[c]	1.40
	T2[1]	37.53 ± 0.33[a]	34[c]	0.91
		38.25 ± 0.38[a]	34[c]	0.89
	T3[1]	2.710 ± 0.00004[a]	8.34[c]	3.08
		2.260± 0.00004[a]	8.34[c]	3.69
		2.190± 0.00004[a]	8.34[c]	3.80
365 A.D. earthquake	**T4[2]**	**0.365[b]**	**9[d]**	24.66

[1]Tiberti et al. (2014); [2]Pirazzoli et al. (1996)
[a]Ages taken from Tiberti et al. (2014).
[b]Ages taken from Pirazzoli et al. (1996).
[c]Present elevation taken from Tiberti et al. (2014).
[d]Present elevation taken from Pirazzoli et al. (1996).
[e]Uplift rate calculated using equation: R = (Ep-E0) / T

Table II.22: Average uplift rate, slip rate, and recurrence time.

Average uplift rate (R) [mm/yr]	Slip rate [mm/yr]	Recurrence time [yr]
2.33	4.66	4291.8

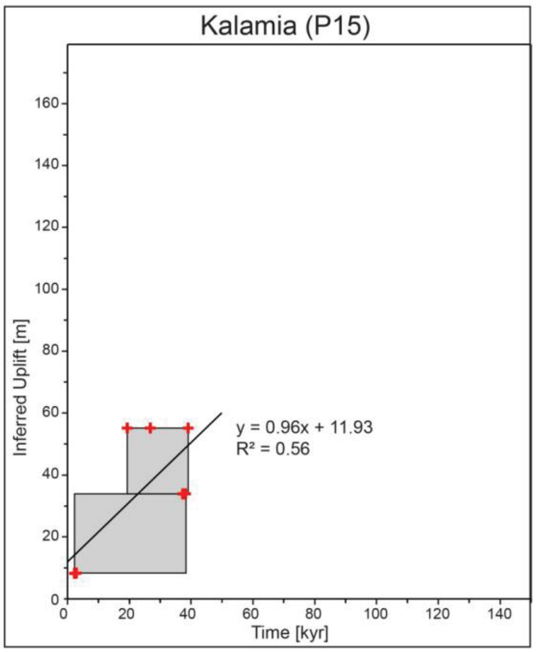

Figure II.35: Inferred uplift diagram curve for tectonic uplift is determined by linear regression analysis.

Table II.23: Displacement between terraces, the corrspnding slip, M_0 and $M_{w.}$

Terraces	Terrace elevation [m]	Terrace elevation [m]	Displacement between terraces [m]	Correspnding slip along the Hellenic trench [m][a]	M_0[b] [dyne/cm]	M_w[c]
T4 – T3	T4 = 9	T3 = 8.34	0.66	1.47	$1.98*10^{27}$	7.5
T3 – T2	T3 = 8.34	T2 = 34	25.66	57.02	$7.7*10^{28}$	8.56
T2 – T1	T2 = 34	T1 = 55	21	46.67	$6.3*10^{28}$	8.47

[a]Corresponding slip along is measured based on the slip of 20 m which equals a vertical displacement of 9 m

[b]Seismic Moment: $M_0 = \mu AD$

[c]Moment Magnitude: $M_w = \frac{2}{3} log M_0 - 10.7$

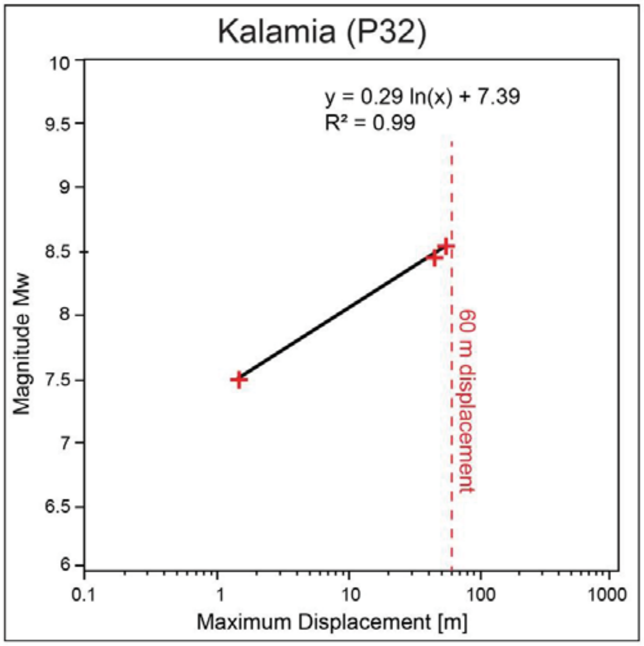

Figure II.36: Regression of maximum displacement versus magnitude Mw. Maximum displacement 60 m ever measured for an earthquake is for the 2011 Mw 9.0 Tohoku-Oki (Japan)

II.1.4.2 Uplift rates only by sea-level changes

Table II.24: Terraces, their age and calculated age, present elevation and sea-level change rate. No tectonics.

Location	Terrace	Time *(T)* $[kyr]$	Elevation present *Ep* [m]	Sea-level change to lower terrace [m]	Sea-level change rate[g] $[\frac{m}{kyr}]$
Kalamia (P32 & H33)	T1[1]	26.93 ± 0.0002[a]	55[c]	-21[e]	0.78
		19.48 ± 0.00009[a]	55[c]	-21[e]	1.08
		39.19 ± 0.0004[a]	55[c]	-21[e]	0.54
	T2[1]	37.53 ± 0.33[a]	34[c]	-25.66[e]	0.68
		38.25 ± 0.38[a]	34[c]	-25.66[e]	0.67
	T3[1]	2.710 ± 0.00004[a]	8.34[c]	+0.66[f]	0.24
		2.260± 0.00004[a]	8.34[c]	+0.66[f]	0.29
		2.190± 0.00004[a]	8.34[c]	+0.66[f]	0.30
365 A.D. earthquake	T4[2]	0.365[b]	9[d]	-9[e]	-24.66
Today shoreline	T5	0	0		

All terraces are dated terraces.
[1]Tiberti et al. (2014); [2]Pirazzoli et al. (1996)
[a]Ages taken from Tiberti et al. (2014).
[b]Ages taken from Pirazzoli et al. (1996).
[c]Present elevation taken from Tiberti et al. (2014).
[d]Present elevation taken from Pirazzoli et al. (1996).
[e]Sea-level fall → -
[f]Sea-level rise → +
[g]Sea-level change rate calculated using equation: sea-level change rate = (height change / age)

II.1.4.3 Uplift rates by tectonic and sea-level changes

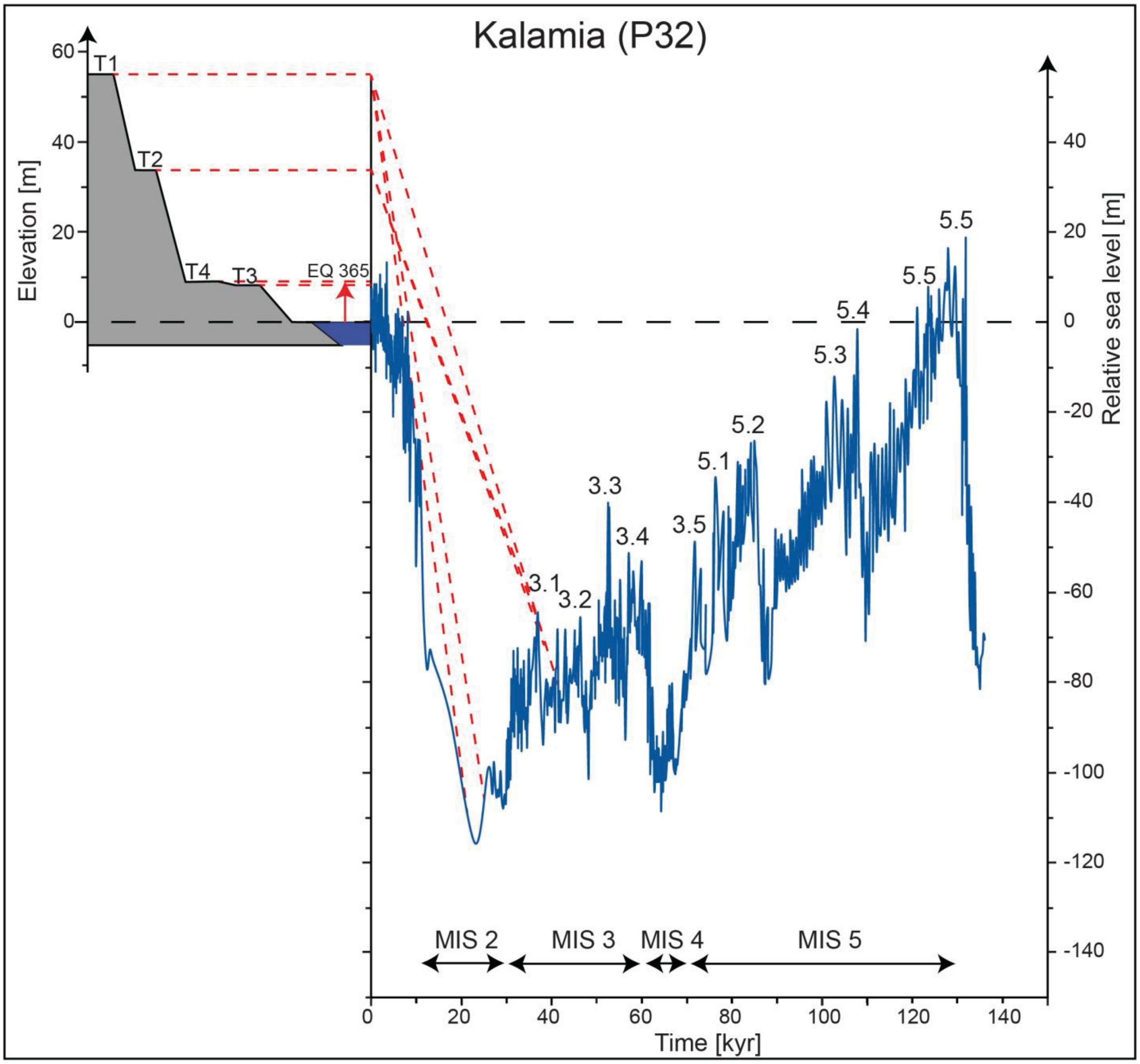

Figure II.37: Correlation of terraces at Kalamia with the sea-level curve of Rohling et al. (2014), modified after Pirazzoli et al. (1996); Tiberti et al. (2014); and Wegmann (2008).

Table II.25: Kalamia terrace numbers, elevation heights, and uplift rates (Rohling et al., 2014).

Location	**Terrace**	**Time *(T)* [*kyr*]**	**Elevation present *Ep* [m]**	**Elevation original *E0* [m]**	$E_p - E_o$ [*m*]	**Uplift rate *(R)*[f] [$\frac{m}{kyr}$]**	**Dated material**
Kalamia (P32 & H33)	T1[1]	26.93 ± 0.0002[a]	55[c]	-103.38±6[e]	158.38±6	5.88±0.22	*
		19.48 ± 0.00009[a]	55[c]	-96[e]	174.4	7.75±0.31	*
		39.19 ± 0.0004[a]	55[c]	-78.76±6[e]	133.76±6	3.41±0.15	*
	T2[1]	37.53 ± 0.33[a]	34[c]	-77.55±6[e]	111.55±6	2.97±0.19	*
		38.25 ± 0.38[a]	34[c]	-92.34±6[e]	126.34±6	3.30±0.19	**
	T3[1]	2.710 ± 0.00004[a]	8.34[c]	0	8.34	3.08	***
		2.260± 0.00004[a]	8.34[c]	0	8.34	3.69	****
		2.190± 0.00004[a]	8.34[c]	0	8.34	3.80	*****
365 A.D. earthquake	**T4[2]**	**0.365[b]**	**9[d]**	**0**	**9**	**24.66**	

All terraces are dated terraces.
[1]Tiberti et al. (2014); [2]Pirazzoli et al. (1996)
[a]Ages taken from Tiberti et al. (2014).
[b]Ages taken from Pirazzoli et al. (1996).
[c]Present elevation taken from Tiberti et al. (2014).
[d]Present elevation taken from Pirazzoli et al. (1996).
[e]Sea-level correction done after Rohling et al. (2014).
[f]Uplift rate calculated using equation: R = (Ep-E0) / T
*Radiocarbon date ^{14}C of a shell (Bivalve fragment) by Tiberti et al. (2014).
**Radiocarbon date ^{14}C of a shell (Glycymeris sp.) by Tiberti et al. (2014).
***Radiocarbon date ^{14}C of a shell (Lithophaga sp.) by Tiberti et al. (2014).
****Radiocarbon date ^{14}C of a shell (Spondylus sp.) by Tiberti et al. (2014).
*****Radiocarbon date ^{14}C of a shell (Vermetids) by Tiberti et al. (2014).

Table II.26: Average uplift rate, slip rate, and recurrence time.

Average uplift rate (R) [mm/yr]	**Slip rate [mm/yr]**	**Recurrence time [yr]**
4.24 ± 0.21	8.48 ±0.42	2358.49 (+122.9 / -111.3)

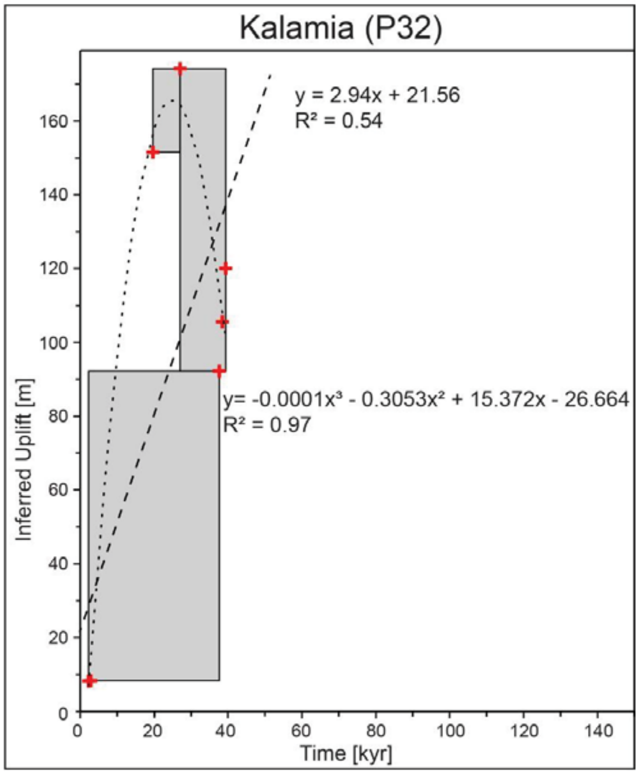

Figure II.38: Inferred uplift diagram curve for sea-level correction is determined by linear regression analysis.

Table II.27: Average uplift rate, slip rate, recurrence time for the 21st July 365 A.D. earthquake, and total slip for highest and oldest terrace at Kalamia.

Earthquake 21st July 365 A.D.	Mw	Time interval [kyr]	Average uplift rate [mm/yr]	Slip rate [mm/yr]	Recurrence time [yr]	Total slip for highest and oldest terrace [m]
Kalamia Tectonic only	8.25[1]	39.19[2] until today	2.33	4.66	4291.8	182.6
Kalamia Constant Sea-level corrected[3]	8.25[1]	39.19[2] until today	4.24±0.21	8.48±0.42	2358.49	332.33

[1] Shaw et al. (2008); [2]Tiberti et al. (2014), [3]Rohling et al. (2014)

II.1.5 Cape Koutouls

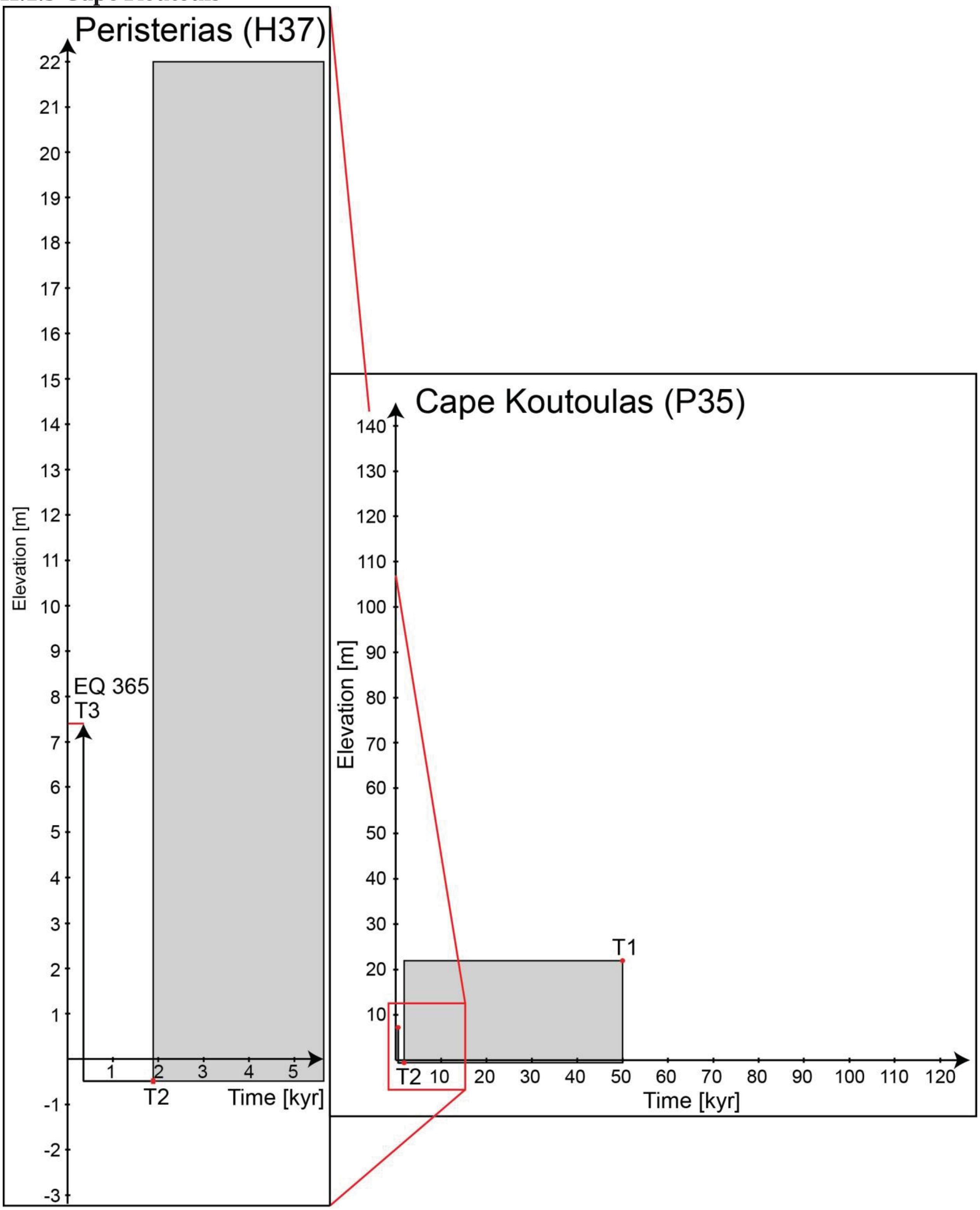

Figure II.39: Elevation of Pleistocene and Holocene paloe-shorelines plotted against time, modified after Wegmann (2008), and Pirazzoli et al. (1996).

II.1.5.1 Uplift rates only by tectonics

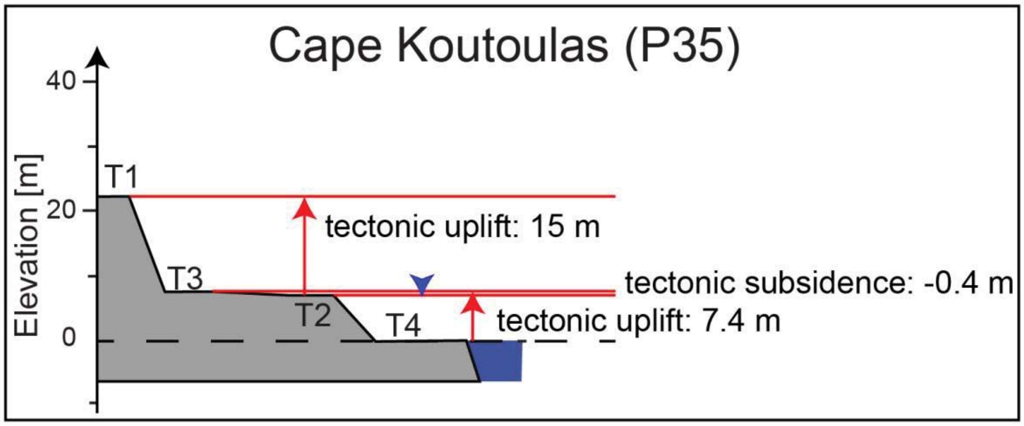

Figure II.40: Elevation of terraces and the height difference needed for the tectonic uplift, , modified after Wegmann (2008), and Pirazzoli et al. (1996).

Table II.28: Terraces, their age, present elevation and calculated uplift rate. No sea-level.

Location	**Terrace**	**Time *(T)* [kyr]**	**Elevation present *Ep* [m]**	**Uplift rate *(R)*[i][$\frac{m}{kyr}$**
Cape Koutoulas (P18 & H37)	T1[1]	50[a]	22[e]	0.44
	T2[2]	**1.890 ± 0.07[b]**	**7.0 ± 0.2[f]**	**3.7 ± 0.24**
	T2[3]	**2.010 ± 0.073[c]**	**7[g]**	**3.5 ± 0.073**
	T2[4]	**1580[d]**	**7[h]**	**4.4**
365 A.D. earthquake	**T3[2]**	**0.365[b]**	**7.4[f]**	**20.27**

[1]Wegmann (2008); [2]Pirazzoli et al. (1996); [3]Price et al. (2002); [4]Mourtzas (2012).
[a]Ages taken from Wegmann (2008).
[b]Ages taken from Pirazzoli et al. (1996).
[c]Ages taken from Price et al. (2002).
[d]Ages taken from Mourtzas (2012).
[e]Present elevation taken from Wegmann (2008).
[f]Present elevation taken from Pirazzoli et al. (1996).
[g]Present elevation taken from Price et al. (2002).
[h]Present elevation taken from Mourtzas (2012).
[i]Uplift rate calculated using equation: R = (Ep-E0) / T

Table II.29: Average uplift rate, slip rate, and recurrence time.

Average uplift rate (R) [mm/yr]	**Slip rate [mm/yr]**	**Recurrence time [yr]**
3.01 ± 0.15	6.02 ± 0.3	3322.3 (+174.2 / -157.7)

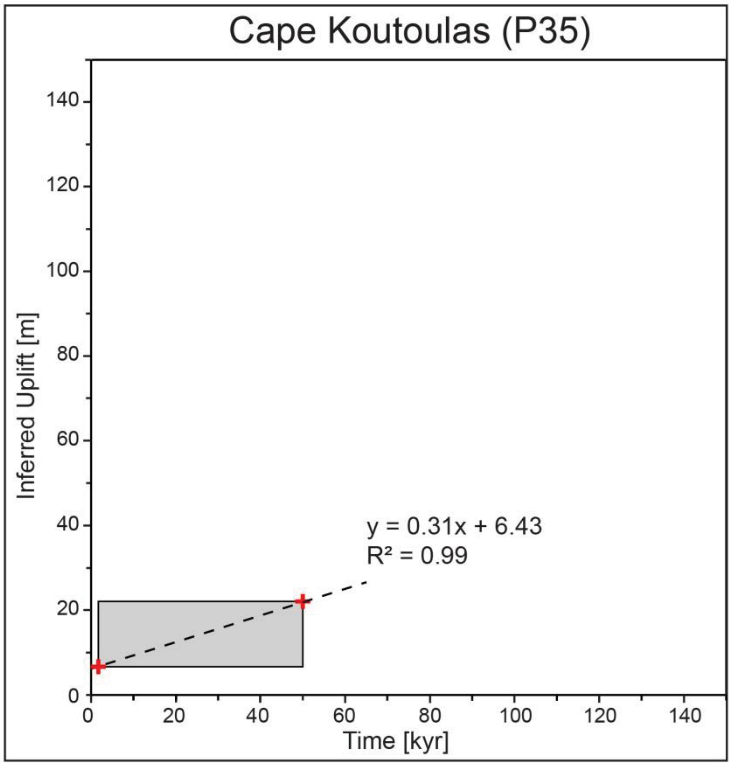

Figure II.41: Inferred uplift diagram curve for tectonic uplift is determined by linear regression analysis.

Table II.30: Displacement between terraces, the corrspnding slip, M_0 and M_w.

Terraces	**Terrace elevation [m]**	**Terrace elevation [m]**	**Displacement between terraces [m]**	**Correspnding slip along the Hellenic trench [m][a]**	**M_0[b] [dyne/cm]**	**M_w[c]**
T3 – T2	T3 = 7.4	T2 = 7	0.4	1.14	$1.54*10^{27}$	7.42
T2 – T1	T2 = 7.0	T1 = 22	15	42.86	$5.7*10^{28}$	8.45

[a]Corresponding slip along is measured based on the slip of 20 m which equals a vertical displacement of 9 m

[b]Seismic Moment: $M_0 = \mu AD$

[c]Moment Magnitude: $M_w = \frac{2}{3} log M_0 - 10.7$

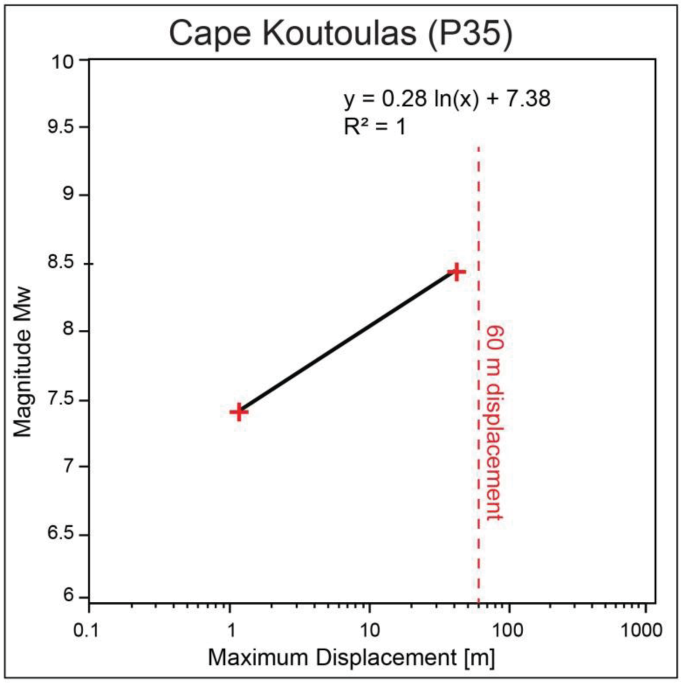

Figure II.42: Regression of maximum displacement versus magnitude Mw. Maximum displacement 60 m ever measured for an earthquake is for the 2011 Mw 9.0 Tohoku-Oki (Japan)

II.1.5.2 Uplift rates only by sea-level changes

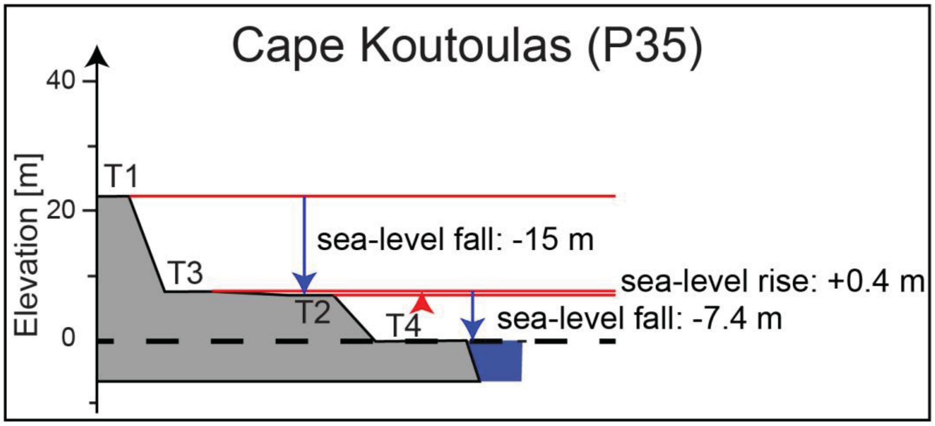

Figure II.43: Elevation of terraces and the needed amount of sea-level fall, modified after Wegmann (2008), and Pirazzoli et al. (1996).

Table II.31: Terraces, their age and calculated age, present elevation and sea-level change rate. No tectonics.

Location	**Terrace**	**Time *(T)*** $[kyr]$	**Elevation present *Ep* [m]**	**Sea-level change to lower terrace [m]**	**Sea-level change rate[k]** $[\frac{m}{kyr}]$
Cape Koutoulas (P18 & H37)	T1[1]	52.5[a]	22[e]	-15[i]	0.28
	T2[2]	**1.890 ± 0.07[b]**	**7.0 ± 0.2[f]**	+0.4[i]	0.21
	T2[3]	**2.010 ± 0.073[c]**	**7[g]**	+0.4[i]	0.19
	T2[4]	**1.580[d]**	**7[h]**	+0.4[i]	0.23
365 A.D. earthquake	**T3[2]**	**0.365[b]**	**7.4[f]**	**-7.4[j]**	**-20.27**
Today shoreline	**T4**	**0**	**0**		

[1]Wegmann (2008); [2]Pirazzoli et al. (1996); [3]Price et al. (2002)); [4]Mourtzas (2012).
[a]Ages taken from Wegmann (2008). MIS ages taken and than converted to ages with Rohling et al. (2014)
[b]Ages taken from Pirazzoli et al. (1996).
[c]Ages taken from Price et al. (2002).
[d]Ages taken from Mourtzas (2012).
[e]Present elevation taken from Wegmann (2008).
[f]Present elevation taken from Pirazzoli et al. (1996).
[g]Present elevation taken from Price et al. (2002).
[h]Present elevation taken from Mourtzas (2012).
[i]Sea-level fall → -
[j]Sea-level fall → +
[k]Sea-level change rate calculated using equation: sea-level change rate = (height change / age)

II.1.5.3 Uplift rates by tectonic and sea-level changes

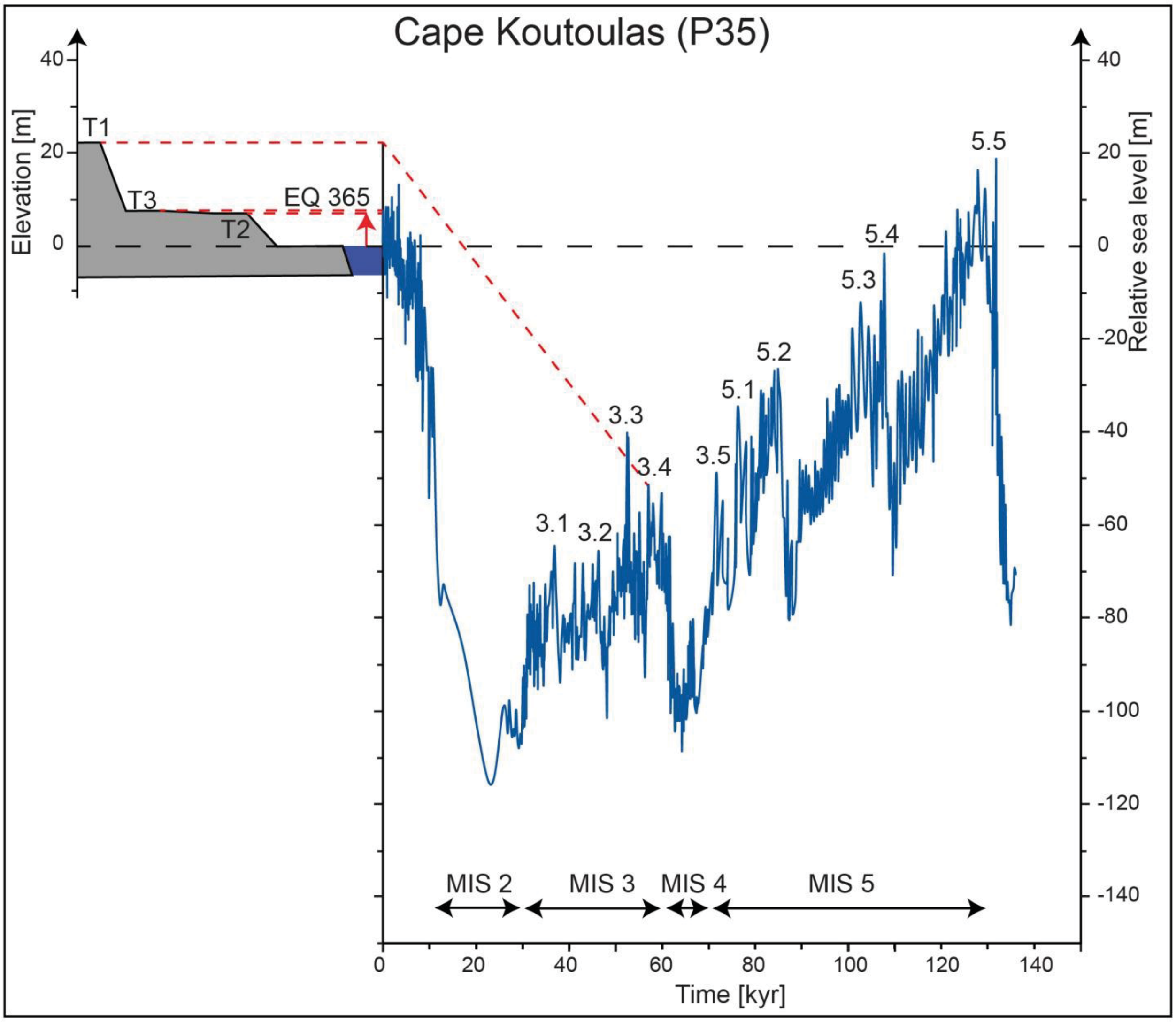

Figure II.44: Correlation of terraces at Cape Koutoulas with the sea-level curve of Rohling et al. (2014), modified after Wegmann (2008), and Pirazzoli et al. (1996).

Table II.32: Cape Koutoulas terrace numbers, elevation heights, and uplift rates (Rohling et al., 2014).

Location	**Terrace**	**Time *(T)*** $[kyr]$	**Elevation present** Ep **[m]**	**Elevation original** $E0$ **[m]**	$E_p - E_o$ $[m]$	**Uplift rate** $(R)^j[\frac{m}{kyr}]$	**Dated material**
Cape Koutoulas (P35 & H37)	T1[1]	52.5[a]	22±1[e]	-55.8±6[i]	77.8 ± 6.08	1.48±0.12	*
	T2[2]	**1.890 ± 0.07[b]**	**7.0 ± 0.2[f]**	**0**	**7.0 ± 0.2**	**3.7 ± 0.24**	**
	T2[3]	**2.010 ± 0.073[c]**	**7[g]**	**0**	**7**	**3.5 ± 0.13**	***
	T2[4]	**1580[d]**	**7[h]**	**0**	**7**	**4.4**	****
365 A.D. earthquake	**T3[2]**	**0.365[b]**	**7.4[f]**	**0**	**7.4**	**20.27**	

Bold terraces are dated terraces.
[1]Wegmann (2008); [2]Pirazzoli et al. (1996); [3]Price et al. (2002); [4]Mourtzas (2012).
[a]Ages taken from Wegmann (2008).
[b]Ages taken from Pirazzoli et al. (1996).
[c]Ages taken from Price et al. (2002).
[d]Ages taken from Mourtzas (2012).
[e]Present elevation taken from Wegmann (2008).
[f]Present elevation taken from Pirazzoli et al. (1996).
[g]Present elevation taken from Price et al. (2002).
[h]Present elevation taken from Mourtzas (2012).
[i]Sea-level correction done after Rohling et al. (2014).
[j]Uplift rate calculated using equation: R = (Ep-E0) / T
*Facies relationship for lateral correlation of spatially separated locations are taken from Wegmann (2008): Facies A - Corresponds to Algal bioherms and patch reefs.
**Radiocarbon date ^{14}C of Dendropoma (Novastoa) petraeum by Pirazzoli et al. (1996). Calculated using a reservoir effect of 320 ± 25 years for the Mediterranean.
***Radiocarbon date ^{14}C of Dendropoma by Price et al. (2002). Corrected the original radiocarbon dates (BP) by adding 430 ^{14}C years to each.
****Mourtzas (2012).

Table II.33: Average uplift rate, slip rate, and recurrence time.

Average uplift rate (R) [mm/yr]	**Slip rate [mm/yr]**	**Recurrence time [yr]**
3.27 ± 0.16	6.54 ± 0.32	3058.10 (+157.33 / -142.65)

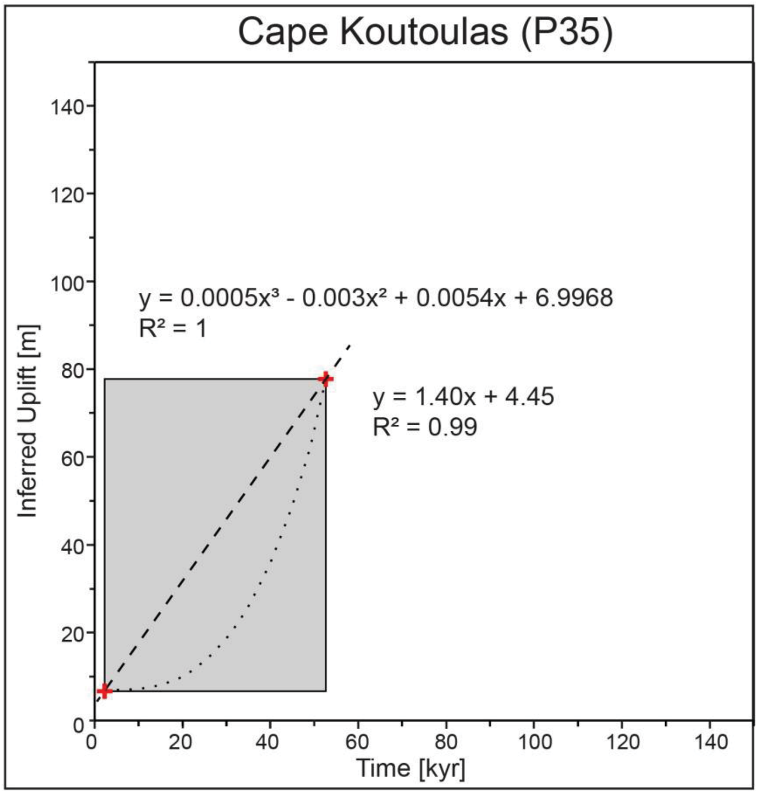

Figure II.45: Inferred uplift diagram curve for sea-level correction is determined by linear regression analysis.

Table II.34: Average uplift rate, slip rate, recurrence time for the 21st July 365 A.D. earthquake, and total slip for highest and oldest terrace at Cape Koutoulas.

Earthquake 21st July 365 A.D.	**Mw**	**Time interval [kyr]**	**Average uplift rate [mm/yr]**	**Slip rate [mm/yr]**	**Recurrence time [yr]**	**Total slip for highest and oldest terrace [m]**
Cape Koutoulas Tectonic only	8.25[1]	50[2] until today	3.01	6.02	3322.3	301
Cape Koutoulas Constant Sea-level corrected[3]	8.25[1]	50[2] until today	3.27±0.16	6.54±0.32	3058.10	343.35

[1] Shaw et al. (2008); [2]Wegmann (2008); [3]Rohling et al. (2014)

II.1.6 Phalasarna

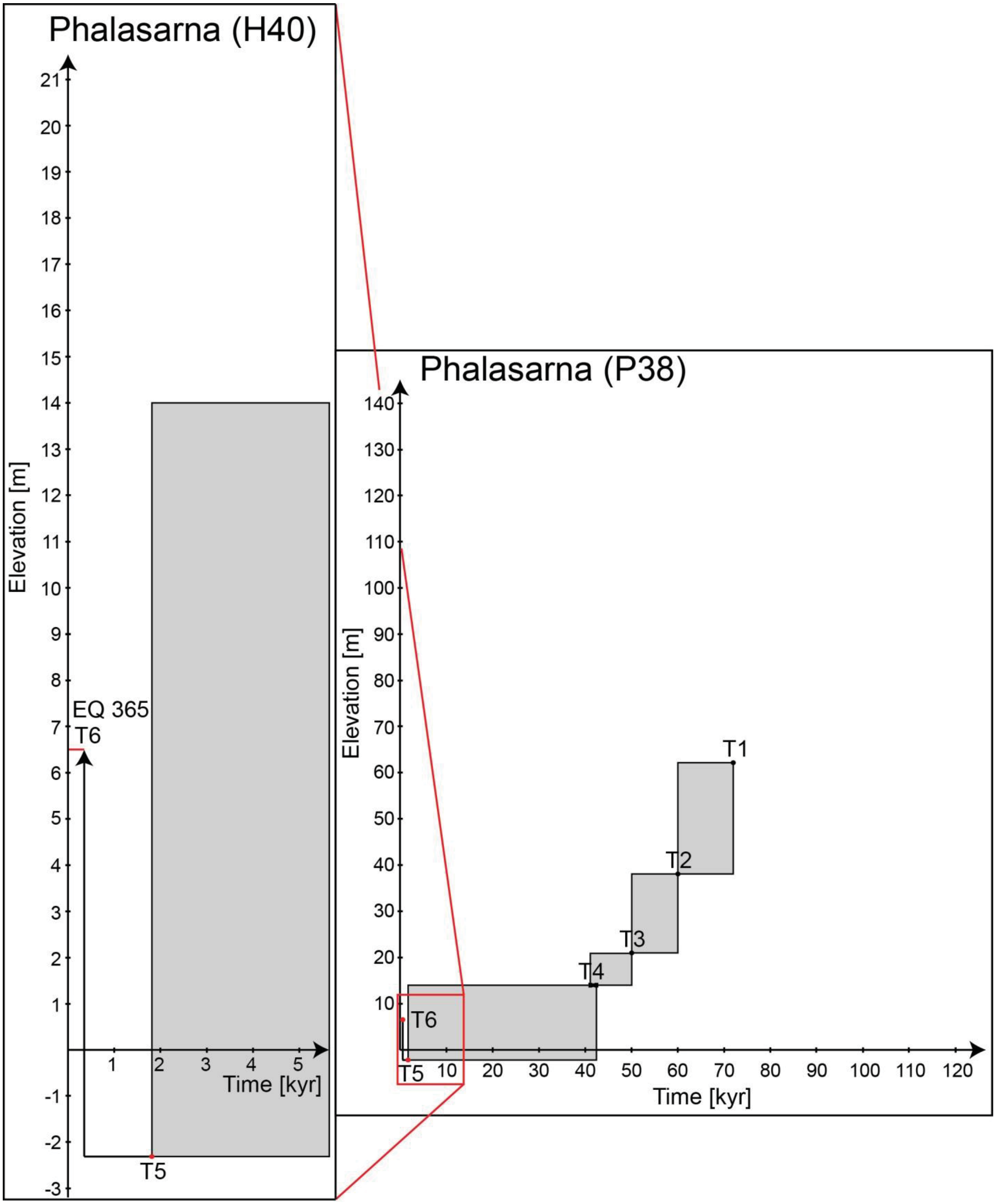

Figure II.46: Elevation of Pleistocene and Holocene paloe-shorelines plotted against time, modified after Wegmann (2008), and Pirazzoli et al. (1996).

II.1.6.1 Uplift rates only by tectonics

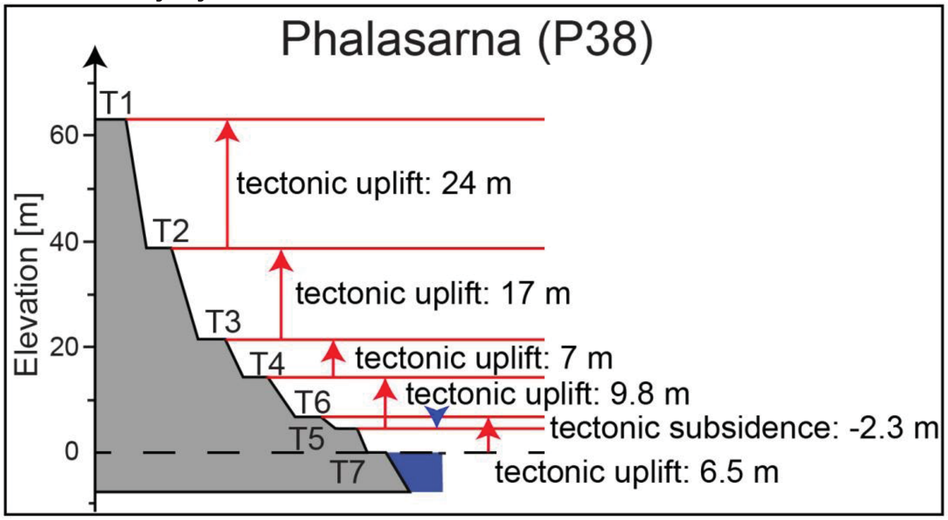

Figure II.47: Elevation of terraces and the height difference needed for the tectonic uplift, modified after Pirazzoli et al. (1996), Wegmann (2008), and Price et al. (2002).

Table II.35: Terraces, their age, present elevation and calculated uplift rate. No sea-level.

Location	**Terrace**	**Time *(T)* $[kyr]$**	**Elevation present *Ep* [m]**	**Uplift rate *(R)*[g] $[\frac{m}{kyr}]$**
Phalasarna (P38 & H40)	T1[1]	72[a]	62[c]	0.86
	T2[1]	60[a]	38[c]	0.63
	T3[1]	50[a]	21[c]	0.42
	T4[1]	**41.28 – 42.53[a]**	**14[d]**	**0.33**
	T5[2]	**1.798 ± 0.077[b]**	**4.2 ± 0.5[e]**	**2.33 ± 0.38**
365 A.D. earthquake	**T6[3]**	**0.365[c]**	**6.5[f]**	**17.81**

[1]Wegmann (2008); [2]Pavlopoulos et al. (2011); [3]Pirazzoli et al. (1996)
[a]Ages taken from Wegmann (2008).
[b]Ages taken from Pavlopoulos et al. (2011).
[c]Ages taken from Pirazzoli et al. (1996).
[d]Present elevation taken from Wegmann (2008).
[e]Present elevation taken from Pavlopoulos et al. (2011).
[f]Present elevation taken from Pirazzoli et al. (1996).
[g] Uplift rate calculated using equation: R = (Ep-E0) / T

Table II.36: Average uplift rate, slip rate, and recurrence time.

Average uplift rate (R) [mm/yr]	**Slip rate [mm/yr]**	**Recurrence time [yr]**
0.91 ± 0.38	1.82 ± 0.72	10989.01(+7192.8 / -3114.9)

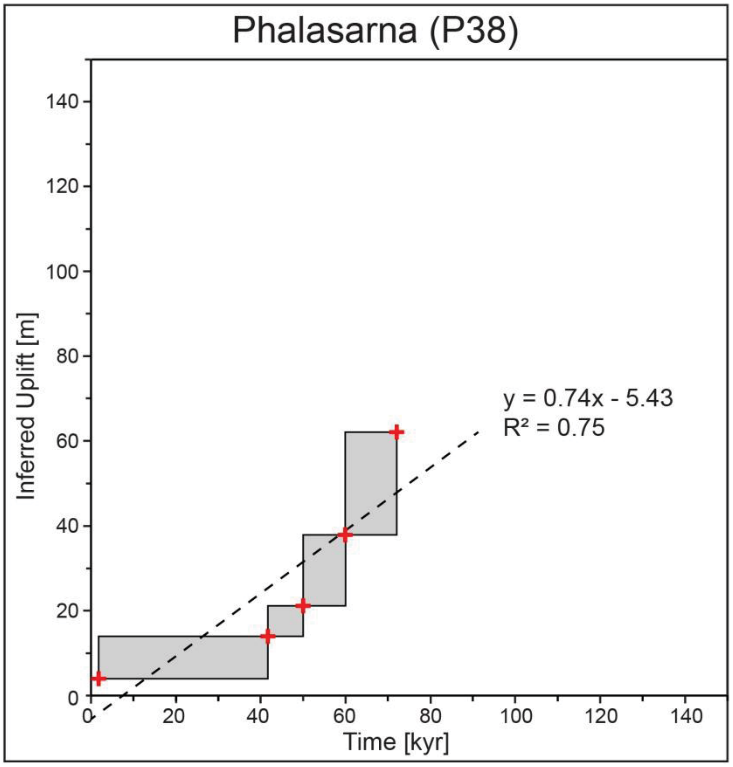

Figure II.48: Inferred uplift diagram curve for tectonic uplift is determined by linear regression analysis.

Table II.37: Displacement between terraces, the corrspnding slip, M_0 and M_w.

Terraces	**Terrace elevation [m]**	**Terrace elevation [m]**	**Displacement between terraces [m]**	**Correspnding slip along the Hellenic trench [m][a]**	**M_0[b] [dyne/cm]**	**M_w[c]**
T6 – T5	T6 = 6.5	T5 = 4.2	2.3	7.07	$9.54*10^{27}$	7.95
T5 – T4	T5 = 4.2	T4 = 14	9.8	42.86	$1.3*10^{28}$	8.02
T4 – T3	T4 = 14	T3 = 21	7	21.54	$2.9*10^{28}$	8.26
T3 – T2	T3 = 21	T2 = 38	17	52.31	$7.1*10^{28}$	8.5
T2 – T1	T2 = 38	T1 = 62	24	73.85	$9.9*10^{28}$	8.6

[a]Corresponding slip along is measured based on the slip of 20 m which equals a vertical displacement of 9 m

[b]Seismic Moment: $M_0 = \mu AD$

[c]Moment Magnitude: $M_w = \frac{2}{3} log M_0 - 10.7$

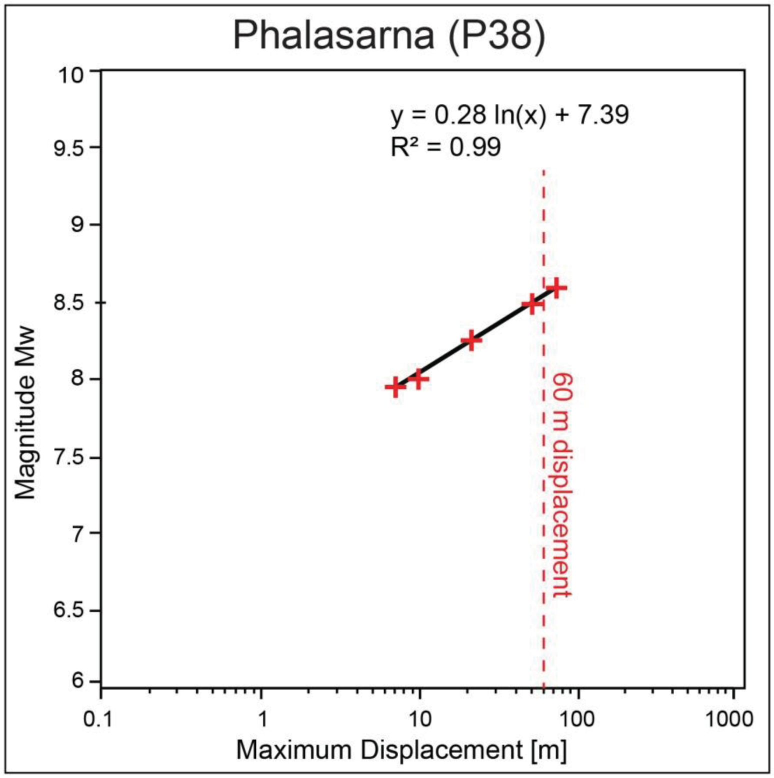

Figure II.49: Regression of maximum displacement versus magnitude Mw. Maximum displacement 60 m ever measured for an earthquake is for the 2011 Mw 9.0 Tohoku-Oki (Japan).

II.1.6.2 Uplift rates only by sea-level changes

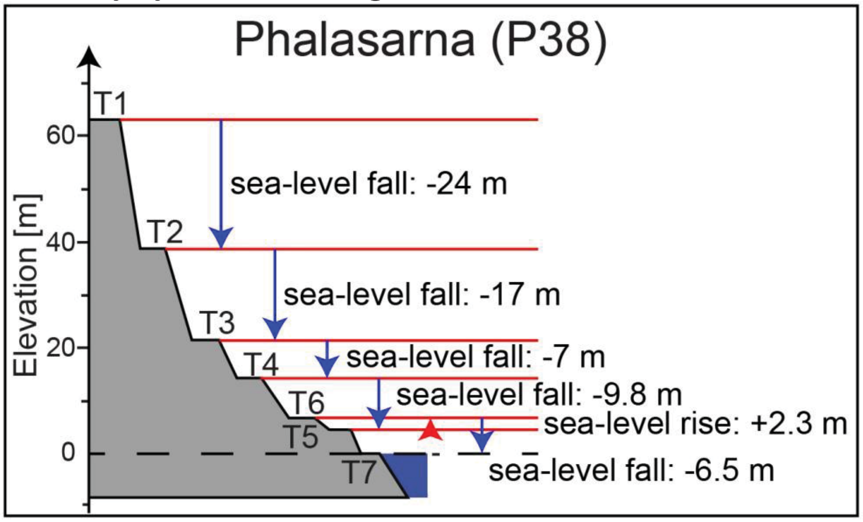

Figure II.50: Elevation of terraces and the needed amount of sea-level fall, modified after Pirazzoli et al. (1996), Wegmann (2008), and Price et al. (2002).

Table II.38: Terraces, their age and calculated age, present elevation and sea-level change rate. No tectonics.

Location	Terrace	Time *(T)* $[kyr]$	Elevation present *Ep* [m]	Sea-level change to lower terrace [m]	Sea-level change rate[j] $[\frac{m}{kyr}]$
Phalasarna (P38 & H40)	T1[1]	71.8[a]	62[e]	-24[h]	0.33
	T2[1]	57[a]	38[e]	-17[h]	0.30
	T3[1]	52.5[a]	21[e]	-7[h]	0.13
	T4[1]	**41.28 – 42.53[b]**	**14[e]**	-9.8[h]	0.23
	T5[2]	**1.798 ± 0.077[c]**	**4.2 ± 0.5[f]**	+2.3[i]	1.28
365 A.D. earthquake	**T6[3]**	**0.365[d]**	**6.5[g]**	-6.5[h]	-17.81
Today shoreline	**T7**	**0**	**0**		

[1]Wegmann (2008); [2]Pavlopoulos et al. (2011); [3]Pirazzoli et al. (1996)
[a]Ages taken from Wegmann (2008). MIS stages taken and corrected the age after Rohling et al. (2014).
[b]Ages taken from Wegmann (2008).
[c]Ages taken from Pavlopoulos et al. (2011).
[d]Ages taken from Pirazzoli et al. (1996).
[e]Present elevation taken from Wegmann (2008).
[f]Present elevation taken from Pavlopoulos et al. (2011).
[g]Present elevation taken from Pirazzoli et al. (1996).
[h]Sea-level fall → -
[i]Sea-level fall → +
[j]Sea-level change rate calculated using equation: sea-level change rate = (height change / age)

II.1.6.3 Uplift rates by tectonic and sea-level changes

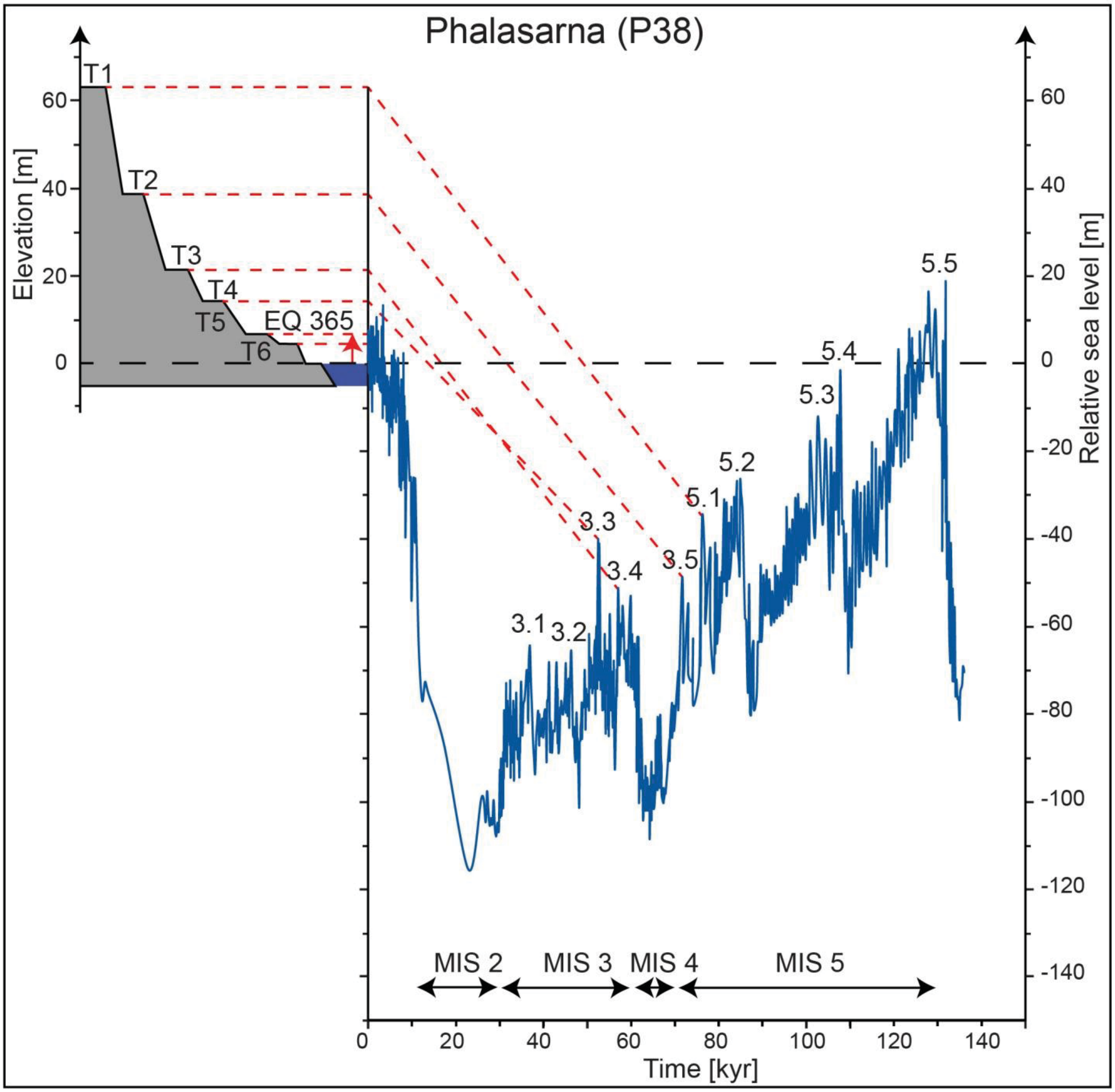

Figure II.51: Correlation of terraces at Phalasarna with the sea-level curve of Rohling et al. (2014), modified after Pirazzoli et al. (1996), Wegmann (2008), and Price et al. (2002).

Table II.39: Phalasarna terrace numbers, elevation heights, and uplift rates (Rohling et al., 2014).

Location	**Terrace**	**Time *(T)*** $[kyr]$	**Elevation present *Ep* [m]**	**Elevation original *E0* [m]**	$E_p - E_o$ $[m]$	**Uplift rate *(R)*[h]** $[\frac{m}{kyr}]$	**Dated material**
Phalasarna (P38 & H40)	T1[1]	71.8[a]	62±1[d]	-53.3±6[g]	115.3 ± 6.08	1.61±0.08	
	T2[1]	57[a]	38±1[d]	-60.9±6[g]	98.9 ± 6.08	1.74±0.11	
	T3[1]	52.5[a]	21±1[d]	-55.8±6[g]	76.8 ± 6.08	1.46±0.12	
	T4[1]	**41.28 – 42.53[a]**	**14**±1[d]	-80.38±6[g]	94.38 ± 6.08	2.27±0.15 to 2.22±0.15	*
	T5[2]	**1.798 ± 0.077[b]**	**4.2 ± 0.5[e]**	**0**	**4.2 ± 0.5**	**2.3 ± 0.38**	**
365 A.D. earthquake	**T6[3]**	**0.365[c]**	**6.5[f]**	**0**	**6.5**	**17.81**	

Bold terraces are dated terraces.
[1]Wegmann (2008); [2]Pavlopoulos et al. (2011); [3]Pirazzoli et al. (1996)
[a]Ages taken from Wegmann (2008). MIS stages taken and corrected the age after Rohling et al. (2014).
[b]Ages taken from Pavlopoulos et al. (2011).
[c]Ages taken from Pirazzoli et al. (1996).
[d]Present elevation taken from Wegmann (2008).
[e]Present elevation taken from Pavlopoulos et al. (2011).
[f]Present elevation taken from Pirazzoli et al. (1996).
[g]Sea-level correction done after Rohling et al. (2014).
[h]Uplift rate calculated using equation: R = (Ep-E0) / T
*Radiocarbon date ^{14}C of bioerosion notch with fringing trottoir-style reef by Wegmann (2008).
**Radiocarbon date ^{14}C of notches, Neogoniolithon by Pavlopoulos et al. (2011).

Table II.40: Average uplift rate, slip rate, and recurrence time.

Average uplift rate (R) [mm/yr]	**Slip rate [mm/yr]**	**Recurrence time [yr]**
1.93 ± 0.17	3.86 ± 0.34	5181.35 (+500.47 / -419.45)

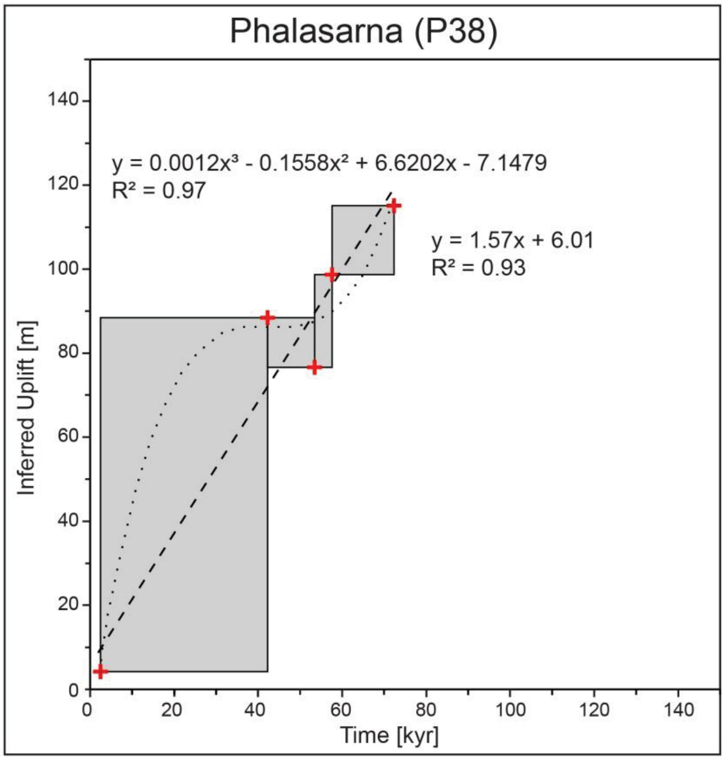

Figure II.52: Inferred uplift diagram curve for sea-level correction is determined by linear regression analysis.

Table II.41: Average uplift rate, slip rate, recurrence time for 21st July 365 earthquake, and total slip for highest and oldest terrace. For tectonic only, sea-level only, and sea-level corrected.

Earthquake 21st July 365 A.D.	**Mw**	**Time interval [kyr]**	**Average uplift rate [mm/yr]**	**Slip rate [mm/yr]**	**Recurrence time [yr]**	**Total slip for highest and oldest terrace [m]**
Aradena Gorge Tectonic only	8.25[1]	107[2] until today	0.75	1.5	13333.33	160.5
Aradena Gorge Sea-level corrected[3]	8.25[1]	107[2] until today	1.37±0.08	2.74±0.16	7299.27	295.65
Sougia Tectonic only	8.25[1]	107[2] until today	1.95	3.9	5128.21	417.3
Sougia Constant Sea-level corrected[3]	8.25[1]	107[2] until today	2.26±0.16	4.52±0.32	4424.78	487.71
Kalamia Tectonic only	8.25[1]	39.19[2] until today	2.33	4.66	4291.8	182.6
Kalamia Constant Sea-level corrected[3]	8.25[1]	39.19[2] until today	4.24±0.21	8.48±0.42	2358.49	332.33
Moni	8.25[1]	85[2]	2.67	5.34	3745.32	453.9

Chryssoskalitissa Tectonic only		until today				
Moni Chryssoskalitissa Constant[3]	8.25[1]	85[2] until today	2.85 ± 0.24	5.7 ± 0.48	3508.77	484.5
Moni Chryssoskalitissa Not Constant[3]	8.25[1]	72[2] until today	2.86 ± 0.25	5.72 ± 0.50	3496.50	410.69
Cape Koutoulas Tectonic only	8.25[1]	50[2] until today	3.01	6.02	3322.3	301
Cape Koutoulas Constant Sea-level corrected[3]	8.25[1]	50[2] until today	3.27±0.16	6.54±0.32	3058.10	343.35
Phalasarna Tectonic only	8.25[1]	72[2] until today	0.91	1.82	10989.01	131.04
Phalasarna Constant Sea-level corrected[3]	8.25[1]	72[2] until today	1.93±0.17	3.86±0.32	5181.35	272.15

[1] Shaw et al. (2008); [2]Wegmann (2008); [3]Rohling et al. (2014)

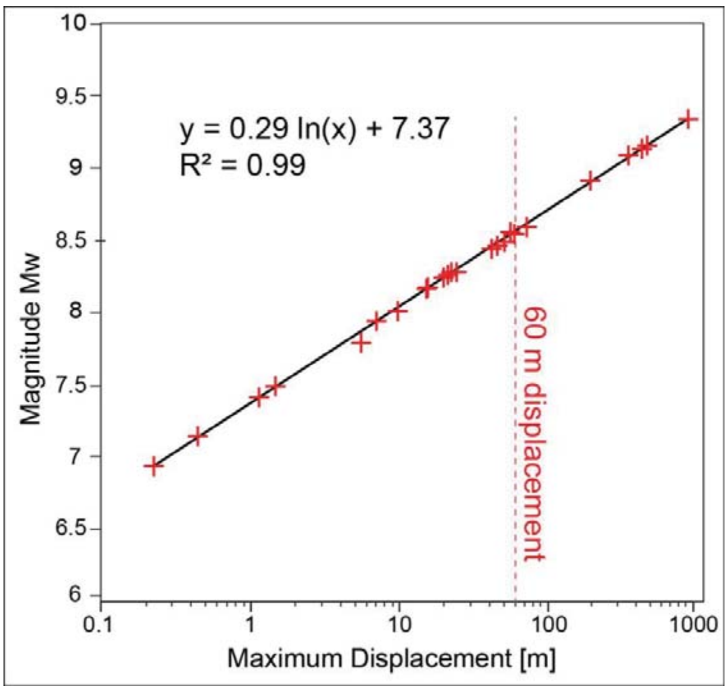

Figure II.53: Regression of maximum displacement versus magnitude Mw. Maximum displacement 60 m ever measured for an earthquake is for the 2011 Mw 9.0 Tohoku-Oki (Japan).

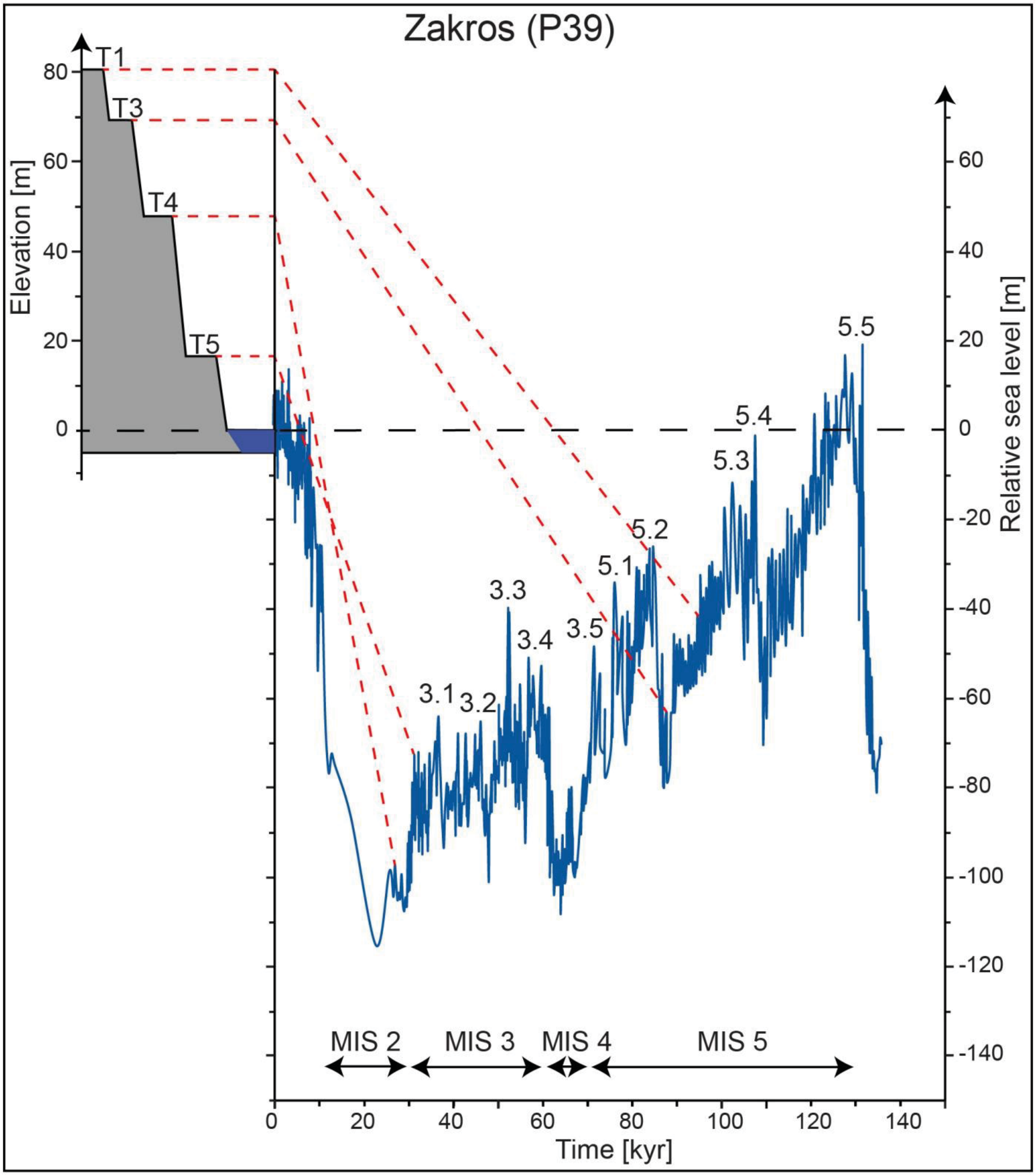

Figure II.54: Correlation of terraces at Zakros with the sea-level curve of Rohling et al. (2014), modified after Strobl et al. (2014).

Table II.42: Zakros terrace numbers, elevation heights, and uplift rates (Strobl et al., 2014; Rohling et al., 2014).

Location	**Terrace**	**Time *(T)*** $[kyr]$	**Elevation present** ***Ep*** **[m]**	**Elevation original** ***E0*** **[m]**	$E_p - E_o$ $[m]$	**Uplift rate** $(R)^1[\frac{m}{kyr}]$	**Dated material**
Zakros (P39)	T1	95±21	81	-42	123	1.3	
	T2	88±22	69	-63	132	1.5	
	T3	27±19	48	-97	145	5.4	
	T4	31±19	17	-72	89	2.9	*

[1]Uplift rate calculated using equation: R = (Ep-E0) / T
*Radiocarbon date ^{14}C of bioerosion notch with fringing trottoir-style reef by Wegmann (2008).
**Radiocarbon date ^{14}C of notches, Neogoniolithon by Pavlopoulos et al. (2011).

Chapter 5

Table II.43: Uplift rates from 16 Ma until 2.58 Ma derived from van Hinsbergen and Meulenkamp (2006).

Number [a]	Mean elevation [m]	Depth[a] [m]	standard deviation [a] [m]	Total height [km]	Age range[a]	Age range[a] [Ma]	Uplift rate[b] [km/Ma]
3	130±30	36		0.166±0.030	U. Serravallian	12	0.014±0.003
4	50±10	935	131	0.985±0.131	U. Serravallian	12	0.082±0.011
5	370±110	36		0.406±0.110	U. Serravallian	12	0.034±0.009
6	260±80	775	207	1.035±0.222	U. Serravallian	12	0.086±0.018
7	10±10	804	136	0.814±0.136	U. Serravallian	12	0.068±0.011
8	210±130	249	168	0.459±0.212	U. Serravallian	12	0.038±0.018
9	150±110	136	14	0.286±0.111	U. Langhian/ l. Serr.	16 to 12	0.018±0.007 to 0.024±0.009
10	360±140	93	35	0.453±0.144	U. Serravallian	12	0.038±0.012
11	280±100	36		0.316±0.100	U. Langhian/ l. Serr.	16 to 12	0.020±0.006 to 0.026±0.008
12	30±10	532	158	0.562±0.158	L. Messinian	5.3	0.106±0.030
12	30±10	496	269	0.526±0.269	L. Pliocene	4 to 3	0.132±0.067 to 0.175±0.090
13	110±30	335	69	0.445±0.075	L. Pliocene	4 to 3	0.111±0.019 to 0.175±0.025
14	150±70	719	92	0.869±0.116		7.1 to 7.4	0.117±0.016 to 0.122±0.016
15	180±60			0.180±0.060			
16	40±20	463	300	0.503±0.301	Messinian	7 to 5.3	0.072±0.043 to 0.095±0.057
17	210±50	743	109	0.953±0.120	U. Tortonian/ l.Messinian	8 to 5.3	0.119±0.015 to 0.18±0.023
18	260±120	624	176	0.884±0.213	U. Tortonian/ l.Messinian	8 to 5.3	0.111±0.027 to 0.167±0.040
19	90±30	1039	85	1.129±0.090	L. Pliocene	4 to 3	0.282±0.023 to 0.376±0.030
20	130±10	636	125	0.766±0.125	U. Tortonian/ l.Messinian	8 to 5.3	0.096±0.016 to 0.145±0.024
21	150±30	609	93	0.759±0.098	U. Tortonian/ l.Messinian	8 to 5.3	0.095±0.012 to 0.143±0.018
22	200±40	605	177	0.805±0.181	U. Tortonian/ l.Messinian	8 to 5.3	0.101±0.023 to 0.152±0.034
23	120±40	831	144	0.951±0.149	L. Pliocene	4 to 3	0.238±0.037 to 0.317±0.050

24	80±40	593	198	0.673±0.202	Pliocene	5.3 to 2.58	0.127±0.038 to 0.261±0.078
25	70±30	372	131	0.442±0.134	U. Tortonian/ l.Messinian	8 to 5.3	0.055±0.017 to 0.083±0.025
26	280±60	183	66	0.463±0.089	U. Tortonian/ l.Messinian	8 to 5.3	0.058±0.011 to 0.087±0.017
27	60±20	784	159	0.844±0.160	L. Pliocene	4 to 3	0.211±0.040 to 0.281±0.053
28	140±40	265	98	0.405±0.106	Messinian	7 to 5.3	0.058±0.015 to 0.076±0.020
29	210±70			0.210±0.070	U. Tortonian/ l.Messinian	8 to 5.3	0.026±0.009 to 0.040±0.013
30	260±120	809	133	1.069±0.179	L. Pliocene	4 to 3	0.267±0.045 to 0.356±0.060
31	10±10	549	171	0.559±0.171	U. Pliocene	4 to 3	0.140±0.043 to 0.186±0.057
32	90±50	59		0.149±0.050	Tortonian	10 to 9	0.015±0.005 to 0.017±0.006
33	130±50	760	91	0.890±0.104	Pliocene	5.3 to 2.58	0.168±0.020 to 0.345±0.040
34	220±80	482	167	0.702±0.185	Pliocene	5.3 to 2.58	0.132±0.035 to 0.272±0.072
35	250±30	87	8	0.337±0.031	U. Tortonian/ l.Messinian	8 to 5.3	0.042±0.004 to 0.064±0.006
35	250±30	902	115	1.152±0.119	L. Pliocene	4 to 3	0.288±0.030 to 0.384±0.040
36	490±50	117	42	0.607±0.065	U. Tortonian	8	0.076±0.008
37	490±70			0.490±0.070	U. Tortonian	8	0.061±0.009
38	70±30	360	80	0.430±0.085	Pliocene	5.3 to 2.58	0.081±0.016 to 0.167±0.033
39	20±20	355	221	0.375±0.222	Pliocene	5.3 to 2.58	0.071±0.042 to 0.145±0.086
40	170±30	362	67	0.532±0.073	Pliocene	5.3 to 2.58	0.100±0.014 to 0.206±0.028
40	170±30	535	284	0.705±0.286	Pliocene	5.3 to 2.58	0.133±0.054 to 0.273±0.111
41	350±130			0.350±0.130	U. Tortonian	8	0.044±0.016
42	80±60	44	13	0.124±0.061	U. Middle Miocene	12	0.010±0.005
43	110±110	83	26	0.193±0.113		4.52	0.043±0.025
44	200±60			0.200±0.060	L. Pliocene	4 to 3	0.050±0.015 to 0.067±0.020
45	340±80	774	217	1.114±0.231	Messinian	7 to 5.3	0.159±0.033 to 0.210±0.044
46	350±50			0.350±0.050		7.05 to 7.95	0.044±0.006 to 0.050±0.007
47	1040±26	82	25	1.122±0.26	U. Tortonian	8	0.140±0.033

	0			1			
47	1040±260	87	47	1.127±0.264	U. Tortonian	8	0.141±0.033
48	220±20	967	77	1.187±0.080	L. Pliocene	4 to 3	0.297±0.020 to 0.396±0.027
49	450±70			0.450±0.070	U. Pliocene	4 to 3	0.113±0.018 to 0.150±0.023
50	380±120	300		0.680±0.120	Messinian	7 to 5.3	0.097±0.017 to 0.128±0.023
51	660±60			0.660±0.060			
52	30±10	158	98	0.188±0.099	U. Pliocene	4 to 3	0.047±0.025 to 0.063±0.033
53	110±50	574	206	0.684±0.212	Pliocene	5.3 to 2.58	0.129±0.040 to 0.265±0.082
54	170±50			0.170±0.050		3.2 to 4.2	0.040±0.012 to 0.053±0.016
55	110±30			0.110±0.030		3.1 to 4.7	0.023±0.006 to 0.035±0.010
56	260±60	100		0.360±0.060	U. Middle Miocene	12	0.030±0.005
56	260±60	200		0.460±0.060	U. Middle Miocene	12	0.038±0.005
57	160±40			0.160±0.040		3.7 to 5.3	0.030±0.008 to 0.043±0.011
58	100±40	531	168	0.631±0.173	Pliocene	5.3 to 2.58	0.119±0.033 to 0.245±0.067
59	230±70			0.230±0.070		3.3 to 4.0 Ma	0.058±0.018 to 0.070±0.021
60	330±30	87		0.417±0.030	U. Pliocene	4 to 3	0.104±0.008 to 0.139±0.010
61	320±40	60	13	0.380±0.042	U. Middle Miocene	12	0.032±0.004
62	70±50	848	285	0.918±0.289	L. Pliocene	4 to 3	0.230±0.072 to 0.309±0.096
62	70±50	389	70	0.459±0.086	Pliocene	5.3 to 2.58	0.087±0.016 to 0.178±0.033
63	270±90	644	165	0.914±0.188	U. Serravallian/ L.Tortonian	12 to 8	0.076±0.016 to 0.114±0.023
64	630±90	694	128	1.324±0.156	U. Middle Miocene	12	0.110±0.013
65	110±30	819	120	0.929±0.124	Tortonian	10 to 9	0.093±0.012 to 0.103±0.014
66	220±160	932	170	1.152±0.233	Tortonian	10 to 9	0.115±0.023 to 0.128±0.026
67	50±50	666	145	0.716±0.153	L. Pliocene	4 to 3	0.179±0.038 to 0.239±0.051
68	20±20	745	283	0.765±0.284	L. Pliocene	4 to 3	0.191±0.071 to 0.255±0.095
69	260±60	699	284	0.959±0.29	Messinian	7 to 5.3	0.137±0.041 to

				0			0.181±0.055
70	340±160	536	161	0.876±0.22 7	Tortonian	10 to 9	0.088±0.023 to 0.097±0.025
71	170±70	1067	130	1.237±0.14 8	lowermost Pliocene	3 to 2.58	0.412±0.049 to 0.479±0.057
73	160±40	1169	35	1.329±0.05 3	lowermost Pliocene	3 to 2.58	0.443±0.018 to 0.515±0.021
74	60±60	1056	37	1.116±0.07 0	lowermost Pliocene	3 to 2.58	0.372±0.023 to 0.433±0.027
74	60±60	823	116	0.883±0.13 1	lowermost Pliocene	3 to 2.58	0.294±0.044 to 0.342±0.0051

[a]: van Hinsbergen and Meulenkamp, 2006
[b]: Uplift rate calculated by R=height/age

CURRICULUM VITAE

08/2013 – 08/2015

Research assistant at the IMF (Remote Sensing Technology institute) of the DLR, Oberpfaffenhofen

Education

09/2008 – 03/2013

Research Assistant in Geology, Department of Earth and Environmental Sciences, LMU Munich

04/2011 – 07/2012

Graduate Student Fellow in the THESIS graduate school of the Bavarian Elite Network Program (University of Munich, Germany).

Since 09/2008

PhD student in Geology, Department of Earth and Environmental Sciences, LMU Munich.

Advisors: Prof. Anke Friedrich (LMU Munich), Prof. Michael Eineder (Technical University Munich, Faculty of Civil, Geo and Environmental Engineering)

02/2007 – 09/2008

Research Assistant in Geology, Department of Earth and Environmental Sciences, LMU Munich

1999 – 2005

'Diploma' (MSc equivalent) in Physical Geography, Department of Earth and Environmental Sciences, LMU Munich, Main subjects: Geophysics and Remote Sensing Diploma thesis: "*Visualization of Synthetic Earthquake Scenarios with a PHP - based interactive Database*". Data of simulated earthquake scenarios of historical earthquakes were visualized for an interactive web page programmed with PHP (Hypertext Preprocessor). Thesis Advisor: Prof. Heiner Igel.

Abstracts

Oral Presentation

Rieger S, Adam N, Friedrich AM (2012): Quantification of crustal deformation based on analysis of Persistent Scatterer Interferometry of W-Crete. EGU2012-9635, presented at 2012 EGU Meeting, Vienna, Austria, 23-27 April.

Rieger S, Adam N, Friedrich AM (2012): Quantifying vertical surface motion on different time-scales, example of Crete, Greece, presented at 14th Symposium on Tectonics, Structural Geology and Geology of Crystalline Rocks, Kiel, Germany, 28-30 March.

Rieger S, Adam N, Friedrich AM (2011): Vertical displacement above a subduction zone (SW Crete): Spatial Coincidence of Co- and Interseismic Surface Uplift – From Historic Data and Persistent Scatterer Interferometry Analysis, presented at 2011 Fragile Earth Meeting. International Meeting, Munich, Germany, 4-7 Sept.

Poster Presentation

Rieger S, Adam N, Friedrich AM (2011): Detection of vertical surface motion using Persistent Scatterer Interferometry of W-Crete, presented at 4th Workshop on Remote Sensing and Geology, EARSel, Mykonos, Greece, 21-24 May.

Rieger S, Adam N, Friedrich AM (2011): Observation of vertical motion above a subduction zone using Persistent Scatterer Interferometry Wide Area Product, SW Crete, Abstract: G23A-0835, presented at 2011 Fall Meeting, AGU, San Francisco, Calif., 5-9 Dec.

Selected Work experience and Internships

06/2005 – 11/2006

Employee at the GAF AG (Company for Applied Remote Sensing), Munich
Involved in monitoring for agricultural subsidy payment of the European Union and in wide-area mapping based on IKONOS satellite images

09/2003

Internship in India at the P.G.S.S (Purvanchal Gramin Seva Samiti) a catholic foreign aid project in Gorakhpur (Uttar Pradesh): Social aid for women, education of children and environmental projects.

08/2003

Internship at the Department of Physics of the Earth at the GFZ Potsdam (German Research Center for Geosciences)
Personal assistant of Prof. Peter Bormann for preparing lectures for seismology using the "IASPEI Manual of Seismological Observatory Practice"

05/2003 – 06/2003

Internship at the DFD (German Remote Sensing Data Center) of the DLR, Oberpfaffenhofen. Involved in the project "Landsat 7 Scientific Data Pool" for geocoding Landsat 7 images, and the project "CORINE Land Cover 2000 (CLC 2000)" statistical comparison of results of CLC 2000 with ministerial data of Germany

11/2002 – 02/2003

Student assistant at the DFD, DLR, Oberpfaffenhofen
Correction of satellite orbit (roll, pitch, and yaw) using "Terrascan" software